UNIVERSITY OF LIVERPOOL

“Are proximal phalangeal fractures in racehorses consistent with a fatigue-type fracture?”

Thesis submitted in accordance with the requirements of the University of Liverpool for the degree of Master in Philosophy by Dr Giulia Lipreri, DVM, MRCVS.

January 2022

Abstract

Fractures of the proximal phalanx are common orthopaedic injuries of racing Thoroughbreds. These fractures are a welfare and an economical concern. Proximal phalangeal fractures occur in a predictable pattern, having a sagittal conformation and extending distally from the sagittal groove of the proximal articular surface of the first phalanx. Debate exists regarding whether these fractures are the result of an acute monotonic overload or of inadequate adaptive response of the bone to exercise.

The aim of this study is to analyse the microstructural characteristics of the subchondral and trabecular bone of the proximal sagittal groove of the proximal phalanx in horses with different training history (racing and non-racing) and injury status (with and without a proximal phalangeal fracture) using micro-computed tomography (μCT).

We hypothesised that microstructural characteristics of the subchondral and trabecular bone of the proximal sagittal groove of the proximal phalanx would vary significantly: (1) across the dorso-to-palmar and medial-to-lateral aspects of the proximal sagittal groove of race-trained horses that have sustained a proximal phalangeal fracture, (2) between race-trained and untrained horses, (3) between race-trained horses that had not sustained proximal phalangeal fracture and race-trained horses that had sustained proximal phalangeal fracture.

Fore limb proximal phalanges were collected from three groups of horses: untrained control group (UC), race-trained control group (TC) and race-trained fracture group (TF). The proximal sagittal groove was resected and imaged with μCT. Eighteen volumes of interest (VOIs) were identified within the subchondral bone (SCB) and trabecular bone (TBB) layers. Each VOI was analysed using a μCT bone analysis software. Tissue mineral density (TMD mg/cm3), was calculated for each VOI within both the SCB and the TBB layer. Total porosity was calculated for VOIs within the subchondral bone only. Bone volume fraction (bone volume/tissue

volume), trabecular thickness (Tb.Th. µm), trabecular separation (Tb.Sp. µm), trabecular number (Tb.N. 1/µm), connectivity density (C.D.), and degree of anisotropy (D.A.) were calculated for each VOI within the trabecular bone layer only. Analysis of variance (ANOVA) and Friedman's test were used respectively for normally and non-normally distributed data to investigate differences between the groups and between VOIs within each group. Significance was set at $p \leq 0.05$.

The study results showed that horses that experienced a proximal phalangeal fracture had higher TMD, higher BV/TV and higher Tb.Th., with lower Tb.Sp., Tb.N. and C.D. compared to horses that did not experience fracture. Moreover, in the TC group, the D.A. is overall significantly higher, compared to both the TF and the UC groups.

In conclusion, an increased subchondral bone TMD along with trabecular thickening and disruption of the trabecular bone architecture, may predispose the horse to proximal phalangeal fracture and may represent an inadequate adaptation to race-training. Our data support previously reported clinical findings suggesting that sagittal proximal phalangeal fractures have characteristics of fatigue-type fracture. This study suggests that sagittal proximal phalangeal fractures occur in horses that respond to race-training by continued bone modelling in the face of suppressed remodeling. Inhibition of remodelling may allow accumulation of fatigue damage that can ultimately result in fracture. Further histological studies are however necessary to confirm the above statement.

Declaration by the author

This thesis is composed of my original work, and contains no material previously published or written by another person except where due reference has been made in the text. I have clearly stated the contribution by others to the thesis.

Contributions by others to the thesis

The majority of the work integrated into this thesis was conducted by Dr Giulia Lipreri. Dr Ellen Singer, Dr Luis Rubio Martínez and Professor Rob van't Hof provided intellectual input on the study design, materials and methods, statistical analysis, interpretation of results, editorial comment and final review on the original research on which the thesis was based.

Table of contents

List of figures

List of tables

List of abbreviations used in alphabetical order

ATP – adenosine triphosphate

BRU – bone remodeling unit

BV/TV – bone volume/tissue volume (bone volume fraction)

C – colt

C.D. – connectivity density

D.A. – degree of anisotropy

DKK-1 – Dickkopf factor 1

F – flat races

G – gelding

IGF – 1 - Insulin-like growth factor 1

LF – left fore limb

M – mare

MCPJ – metacarpophalangeal joint

MC3 – third metacarpal bone

NH – national hunt races

NO – Nitric Oxide

OPG – osteoprotegerin

PGE_2 – Prostaglandin E2

PP – proximal phalanx

PSBs – proximal sesamoid bones

PSG – proximal sagittal groove

RANKL – receptor activator of nuclear factor Kappa-B ligand

RF – right fore limb

SCB – subchondral bone

TBB – trabecular bone

Tb.N. – trabecular number

Tb.Sp. – trabecular separation

Tb.Th. – trabecular thickness

TMD – tissue mineral density

WNT – Wingless-related integration site

Chapter 1

Introduction

Fractures of the proximal phalanx (PP) are common orthopaedic injuries of racing Thoroughbreds. These fractures, as most of the musculoskeletal injuries of racehorses, are a welfare and an economical concern. Proximal phalangeal fractures occur in a predictable pattern, having a parasagittal conformation and extending distally from the sagittal groove of the proximal articular surface of the first phalanx (Smith 2014a, Ellis 1987, Markel 1985). However, etiopathology of PP fractures is still a matter of discussion. Debate exists whether sagittal fractures of the PP are the result of an acute monotonic overload or of inadequate adaptive response of the bone to exercise.

This study analyses and compares microstructural and anisotropic characteristics of the subchondral bone (SCB) and trabecular bone (TBB) of the proximal sagittal groove of the PP in horses with different training history (racing and non-racing horses) and injury status (horses with and without sagittal fractures of PP) by use of micro-computed tomography. The ultimate objective of the study is to better understand the role that inadequate adaptive response of bone to exercise contributes to sagittal fractures of the PP.

Chapter 2 reviews the current literature relating to bone biology with particular focus on bone modeling/remodeling and on bone adaptation to exercise. Also included is a review of the literature on PP fractures.

Chapter 3 details the materials and methods, as well as the statistical analysis, used to obtain our final data.

Chapter 4 details the results obtained from the analysis of our data.

Chapter 5 provides a general discussion of the results, lists the main limitations of the study and recommends future directions of research.

References cited in the MPhil are listed at the end of the thesis.

Chapter 2

Literature review

2.1 Equine Skeleton

The main role of the mammalian skeleton is to provide structural support and a means of locomotion using jointed bones stabilized and moved by ligaments, tendons and muscles. The bony skeleton also provides protection for vital organs and a reservoir of minerals. The skeleton has evolved to provide maximum strength with minimal mass. The shape and size of individual bones are determined by genetic and functional factors to provide appropriate structure for functional demand with a low risk of failure and without incurring excess energy expenditure. The demands for energetic efficiency are greater in animals evolved for high-speed locomotion, such as horses. The horse is an unguligrade animal, standing on the hoof of the third digit. The distal end of the limb has evolved to form a hoof. The major muscle masses of the equine limbs are positioned proximally to reduce the energy required to move the limb as it swings backward and forward in cursorial locomotion. Bone mass is also minimized at the distal extremities and safety margins decrease toward the distal extremity of the limbs (Sinclair et al. 2014).

The horse has evolved to become a high-speed animal and has also been the subject of selective breeding as an elite animal athlete. The Thoroughbred racehorse is a prime example of selection for speed. However it is suggested that this selection process might have reached its limit (Hill et al. 1988, Bailey et al. 2022). Despite the efforts of breeders, the winning times of Thoroughbreds in the English classic horse races have not fallen substantially over the past 50 years. In men and women's track events, new records are set almost yearly. In the Olympic games, for example, the time taken for men to run 1500 metres declined by 15 seconds (7%) from 1936 to 1984. These improvements cannot be attributed to genetic change, but to better training, health, tracks, and wider screening of the population. Unfortunately, equine sport science is not yet developed or applied to the same extent as in human athletics**.** Both human

and equine skeleton has the capacity to respond to changes in mechanical loading in the short term and can optimize for energetic efficiency in relation to changes in mechanical demands (Sinclair et al. 2014).

2.2 Bone as a tissue

The skeleton is a metabolically active organ, which is composed of water (10%), inorganic material (65%) and organic material (25%) (Burr and Akkus 2014). The inorganic component, primarily hydroxyapatite, imparts high compressive strength. The organic matrix of bone consists largely of type I collagen (approximately 90%), with small amounts of lipid and non-collagenous proteins. The fibrous protein collagen imparts high tensile strength. Non-collagenous proteins within the bone matrix include signalling molecules (such as transforming growth factor beta and insulin-like growth factor I) and regulators of mineralization (such as osteocalcin and dentin matrix protein) (Sims and Martin 2019). Adult bone tissue comprises three major populations of cells: osteoblasts, osteoclasts and osteocytes. Osteoblasts are derived from stromal mesenchymal cells present in the bone marrow. There are cells at different stages of differentiation within the mesenchymal "osteoblast lineage" that perform a wide range of functions: bone collagen matrix production, regulation of mineralization and osteoclastogenesis, production of paracrine and autocrine factors (cytokines, growth factors, prostanoids, proteinases). The osteoblast lineage forms communication systems profoundly influencing bone formation, bone resorption and haematopoiesis (Sims and Martin 2020). Osteoclasts are derived from circulating monocytes (haematopoietic origin), are multi-nucleated and form through fusion. The main function of osteoclasts is bone resorption. When activated, osteoclasts reside on a bone surface with a ruffled border and create acidic resorption lacunae. Osteoclasts secrete hydrochloric acid to

418 dissolve hydroxyapatite, as well as secreting Cathepsin K to degrade type I collagen (Takahashi
419 et al. 2019). Osteocytes are osteoblasts that became entrapped within the bone matrix during
420 bone formation. These cells make up 90-95% of all bone cells in the adult skeleton and are
421 recognized as the major orchestrator of bone homeostasis, including mechanical sensing and
422 transducing mechanical signals into chemical signals to regulate both bone formation and
423 resorption during remodeling (Schaffler et al. 2014). Bone remodeling is a crucial process to
424 maintain a balance of bone homeostasis. Osteocytes regulate bone remodeling in direct and
425 indirect ways. Osteocytes sense the mechanical stimuli based on changes in stress and strain
426 in the bone , which directs their job of orchestrating the activity of osteoblasts and clasts. As
427 a consequence, osteocytes indirectly regulate bone resorption and bone formation, resulting
428 in a balance of bone homeostasis (Robling and Bonewald 2020). Osteocytes control
429 osteoclastogenesis by stimulating Receptor Activator of Nuclear Factor Kappa-B Ligand
430 (RANKL - molecule responsible of osteoclast differentiation) expression and/or availability,
431 and by inhibition of osteoprotegerin (OPG - inhibitor of osteoclast differentiation) expression
432 and/or availability (Cao et al. 2020). Osteocytes also regulate osteoblast activity by producing
433 both inhibitory (Sclerostin and Dickkopf factor 1) and stimulatory (Prostaglandin E_2, Insuline-
434 like growth factor 1, Wingless-related integration site glycoproteins, Nitric Oxide free radical
435 and Adenosine Triphosphate Nucleotide) factors. Mechanical stimulation can induce secretion
436 of both stimulatory and inhibitory molecules by the osteocytes (Cao et al. 2020). Depending
437 on the position within a loaded bone, some osteocytes stimulate bone formation whilst in
438 other locations inhibition takes place. This results in change of bone shape.
439
440
441

2.3 Bone modeling and remodeling

Both during growth and maturation and in the skeletally mature adult, bone responds to mechanical loading. Bone is also the main store of calcium and phosphate in the body, and bone metabolism regulates calcium and phosphate homeostasis. The relationship of the pathophysiology of functional adaptation to training and conditioning regimens in general, and in the horse in particular, is important in maximizing performance and minimizing skeletal injury.

Skeletal morphology is determined by two processes: modeling and remodeling. Bone modeling describes the process by which bones are shaped or reshaped by the independent action of osteoblasts and osteoclasts. In bone modelling, the activities of osteoblasts and osteoclasts are not necessarily coupled spatially or temporally, as is the case in bone remodeling. Bone modeling defines skeletal development and growth and is responsible for the shaping of bones. Modeling includes both formation and resorption of bone. Bone formation takes place from the beginning of skeletogenesis during foetal life until the time when the longitudinal growth of the skeleton is completed. Modeling is also responsible for changes in bone shape associated with aging or in response to mechanical load. A change in bone shape is seen, for example, in tennis players where the arm used to hold the racket has a higher bone mass than the other arm (Kontulainen et al. 2002). In remodeling, the actions of osteoblasts and osteoclasts occur in sequence on the same bone surface. Remodeling occurs asynchronously throughout the skeleton at many anatomically distinct sites termed bone remodeling units (BRUs). Remodeling persists throughout life. In humans, it has been estimated that 3–4 million BRUs are initiated each year and that 1 million BRUs are actively engaged in bone turnover at any time (Manolagas 2000). Remodeling is a process characterized by four phases: the activation phase when the osteoclasts are recruited; the

resorption phase, when the osteoclasts resorb bone; the reversal phase, in which the osteoclasts undergo apoptosis or become inactive, and the osteoblasts are recruited; and the formation phase, where the osteoblasts lay down new organic bone matrix that subsequently mineralizes. The purposes of remodeling are many, including calcium homeostasis and the replacement of old and damaged bone with new bone, essentially repair of damaged bone. By removing old and damaged bone, targeted remodeling plays a key role in maintaining the mechanical strength of bone; however, excessive remodeling and repair poses a risk to bone strength as it destabilizes bone and introduces stress concentrators (Einhorn 1992). Even targeted remodeling may be harmful according to the hypothesis that excessive strain causes regional microdamage, which leads to targeted remodeling removing the damaged bone and a larger volume of the surrounding undamaged bone. The temporary bone volume deficit increases the strain in neighbouring bone and the potential establishment of a vicious cycle between damage and repair (Allen and Burr 2008; Martin 1995). On the other hand, remodeling has an important role in prolonging the fatigue life of a given volume of bone by replacing bone that has accumulated microdamage (Taylor et al. 2004). Bone remodeling rates are reduced during conditions of sustained high-magnitude cyclic loading and microdamage accumulating (Jee et al 1990, Jee et al. 1991). This phenomenon is observed in Thoroughbred racehorses in training (Whitton et al. 2010). At sites of high bone density known to be subjected to high loads, such as the third metacarpal bone dorsal cortex and the subchondral bone of the palmar aspect of the third metacarpal condyles, decreased porosity and fewer resorption surfaces are observed when horses are in training compared with those that are resting from training (Riggs et al. 1999).

2.4 Bone Organization

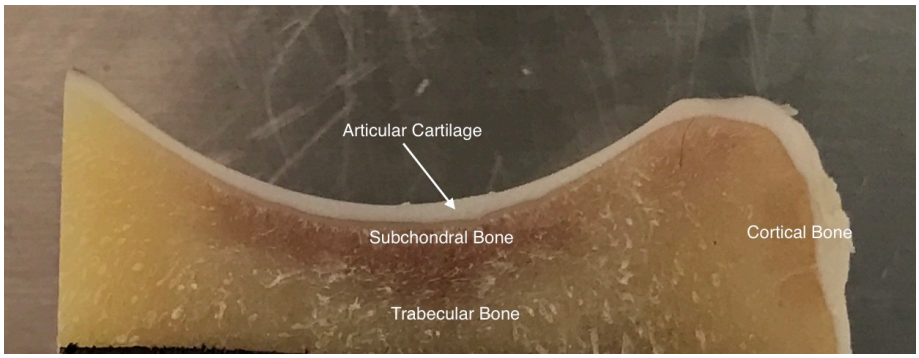

Figure 1: Sagittal section of the proximal aspect of the proximal phalanx showing the cortical and trabecular bone.

Macroscopically, the bone is organized in cortical bone and trabecular bone (Figure 1). Cortical bone is the primary component of the shafts and diaphysis of long and short bones of the extremities. Cortical bone is also found surrounding trabecular bone of vertebral bodies and cuboidal bones, at the metaphysis of long bones and in the skull. Trabecular bone is found primarily in the metaphysis of the long bones, as well as in the vertebrae, ribs and iliac crest. Trabecular bone derives its primary mechanical benefit from its architecture, which provides structural support without increasing weight of the entire bone. One important mechanical function of the trabecular bone is to provide a means for the bone to funnel the stresses imposed on it to the stronger cortical bone. The architecture of the trabecular bone can be characterized by Trabecular Number (Tb.N.), Trabecular Thickness (Tb.Th.), Trabecular Separation (Tb.SP.) and degree of interconnection (Connectivity Density – C.D.).

As a composite material, bone matrix is anisotropic meaning that its structural orientation and mechanical properties change depending on the direction of load application. Bone is strongest in compression, weaker in shear and weakest in tension. The architecture of the

matrix in relation to the osteocytes forms the basic unit of structure, termed the lamella (Figure 2).

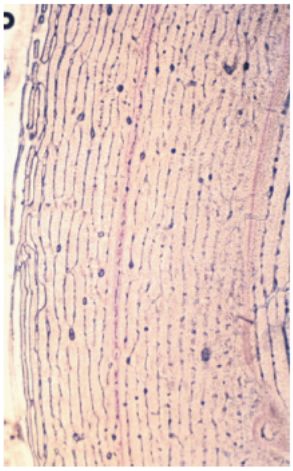

Figure 2: Photomicrograph of a transverse section of laminar bone. From: Skeletal physiology: responses to exercise and training. In: "Equine Sports Medicine and Surgery". Eds. Hinchcliff, K.W., Kaneps, A.J., Geor, R.J. 2nd ed. Elsevier).

The architecture of these bone lamellae in different geometrical arrangements forms the basis of the different histological types of bone. In cortical bone, concentric circumferential lamellae form osteons and when these are formed in the original development of the bone they are termed 'primary osteons'. A similar architecture is also seen in the secondary osteons that are formed to repair damage such as microcracks. Lamellae formed around vascular networks or plexi result in laminar or the less regular plexiform bone often seen in ungulates like the horse. This type of bone allows very rapid increases in cross-sectional area with later consolidation (Currey 2001). Lamellar bone can also form circumferential lamella on the entire periosteal and endosteal surfaces of individual bones. The trabecular bone is formed by "plates and rods" of bone and are formed of aligned bone lamellae. The plates and rods are strategically arranged in relation to the trajectories of principal compressive and tensile stresses. In embryological development and in the early stages of fracture repair a rapidly forming bone

529 with irregular lamellae, coarse collagen fibres and large osteocyte lacunae is seen. This is
530 called ‘woven’ bone and is rapidly remodeled to the various types of organized lamellar bone,
531 such as primary and secondary osteonal bone. Bone morphology has been related to the
532 mechanical loading requirements of different specific bones. For example, the orientation of
533 collagen fibers in the cranial and caudal cortices of the radius reflects the mechanical
534 requirements of this bone. Strain gauge studies have shown that this bone is loaded in both
535 compression and bending with principal tensile strains aligned with the long axis of the bone
536 in the cranial cortex and principal compressive strains aligned to the long axis in the caudal
537 cortex (Biewener et al. 1983). The arrangement of collagen fibers in relation to this pattern of
538 loading has been demonstrated by Riggs et al. (1993). This has been supported by a
539 comprehensive analysis of matrix morphology in the equine radius, in which the analysis of
540 primary bone and bone within secondary osteons of the cranial and caudal cortices of the
541 radius were arranged appropriately to optimize for the pattern of functional loading (Mason
542 et al. 1995). This study also confirmed a predominant longitudinal arrangement of collagen
543 fibers in the cranial cortex of this bone, to resist the functional tensile strains at this location.
544 Any consistent changes in the magnitude and pattern of loading induce a modeling response
545 in which the bone cell activity will modify the matrix to maintain the optimization of the overall
546 bone architecture in relation to the new prevailing loading conditions. Matrix, and embedded
547 osteocytes, can be removed by osteoclasts and new matrix formed by osteoblasts. This
548 coupled cellular activity allows bone as both a material and structure to be changed in terms
549 of mass and distribution throughout life.
550
551
552

2.5 Skeletal biomechanics

The mechanical properties of bone are determined by size, shape, and internal structure as well as composition. When a force is applied to a bone, deformation of the structure occurs. The response of bone to application of external forces called loads is used to quantify specific measures of mechanical behaviour. When testing the structural properties of a bone, the relationship between load and displacement can be represented graphically on a load-deformation curve (Figure 3).

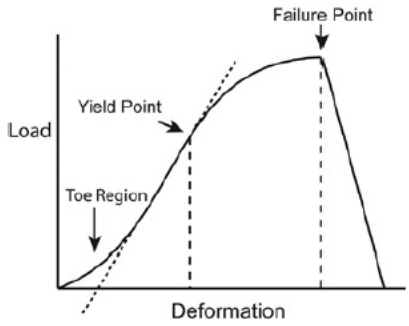

Figure 3: Load-deformation curve (From Bone biology and fracture healing. In: "Equine Surgery". Eds: Auer J.A and Stick J.A. 5th ed. Elsevier, Sounders, St Louis, Missouri.)

The initial curved segment of the curve is the toe region, a low-force, high-deformation region that reflects tissue fluid motion as well as straightening and stretching of protein fibres such as collagen and elastin. The following linear segment of the curve is the elastic region and shows the ability to resist deformation. In this region, the structure will return to its original form when the load is removed. This section of the curve is often referred to as the stiffness. It is critical to understand that the stiffness refers to the composite structure or construct and depends on the shape and interaction between separate components. As loading continues through the elastic region, the yield point is reached, beyond which permanent deformation occurs in the plastic segment of the curve. That is, the structure will not return to its original

shape when the load is removed. The amount of plastic deformation, like elastic deformation, depends on the applied load. With increasing load, the bone will eventually undergo significant plastic or irreversible deformation at a load and deformation defined as the failure point. The ultimate load is the load beyond which the structure essentially loses all capacity to withstand increasing forces. The ultimate load may be identical to or higher than the failure load. Taken together, the information on a load-deformation curve largely depends on the sample configuration and the relative orientation of the load (Lopez 2019).

To assess the mechanical behaviour of a material, the force-deformation relationship is normalized by dividing the applied force by the cross-sectional area (stress, σ) and the deformation by the original length (strain, ε) to eliminate the influence of the structure's geometry. Material properties may be of greatest interest in investigations surrounding the properties of fracture callus or the effects of exercise or diet on bone. For material properties testing, areas of interest are typically included in specimens prepared from larger structures. The specimens are generally identical in size, shape, and microstructural orientation. As indicated earlier, the testing process may be very similar to the testing of structural properties, but the load and deformation data are stress and strain, respectively.

Stress (σ) is the intensity of the force divided by the area that it acts upon. Common stress units include pounds per square inch (psi) and pascals (Pa). Strain (ε) is the change in dimension divided by the original dimension. A stress-strain curve typically looks very similar to a load-deformation curve with stress on the ordinate versus strain on the abscissa (Figure 4). The slope of the elastic segment of the stress-strain curve is called Young's elastic modulus when the stress is normal, and the strain is proportionately linear to the applied stress. The slope is the shear modulus when the stress is primarily shear. The yield and failure points are similar to those described earlier, with notable exceptions of the units and that they represent

material versus structural properties. Additionally, the ultimate stress and strain may be different from the failure stress and strain. The yield or failure energy is dissipated when the structure yields (yield strength) and then fails (failure strength).

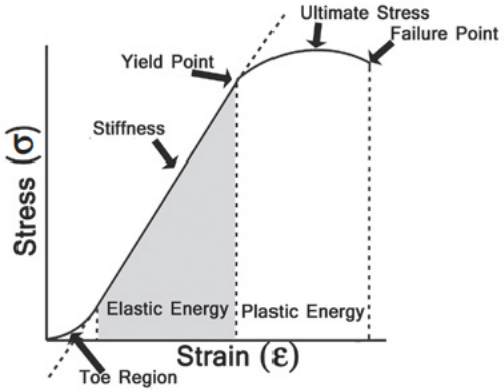

Figure 4: Stress-strain curve typical of a bone sample. (From Bone biology and fracture healing. In: "Equine Surgery". Eds: Auer J.A and Stick J.A. 5th ed. Elsevier, Sounders, St Louis, Missouri).

When a crack starts to form, energy is released as two new surfaces are created. If the amount of energy released is less than that required to form the crack, the crack will stop. Otherwise, the crack will continue to spread and more cracks will form, consistent with catastrophic failure. The more energy stored in a bone prior to failure, the greater the comminution and/or soft tissue damage that will be caused when a fracture occurs. A number of material properties can be derived from a stress-strain diagram. A higher elastic modulus indicates a stiffer material that has higher resistance to deformation. Compliance is the opposite of stiffness. The terms "ductile" and "brittle" describe the area under the stress-strain curve and represent the toughness of a material. Toughness is the capacity of a material to sustain deformation without failure. A larger area under the curve indicates a tougher material. A ductile material has extensive plastic deformation and high-energy absorption prior to failure.

A brittle material, like glass, has a sudden failure without any considerable plastic deformation and comparably low-energy absorption. The ability of the material to store or absorb energy without permanent deformation is the resilience of the material. The modulus of resilience is equal to the area under the stress-strain curve in the elastic region. Cortical bone is more brittle than trabecular bone and fails at lower strain, albeit a higher load. Trabecular bone stores more energy prior to failure compared with cortical bone, owing to higher toughness. As bone deforms, it stores the applied energy as strain energy. The energy is released when the bone fractures. Due to its microstructure, bone is stiffer when loaded at a faster rate, and hence it stores more energy prior to failure at a faster compared to a slower loading rate. Therefore, a bone loaded rapidly fails at a higher load and releases more energy than if it is loaded slowly (Lopez 2019).

Fractures can occur as a result of a single load beyond the failure point or repeated loads below the failure point. Bones that fail from repeated cyclic loading are typically viewed as failing secondary to fatigue. The resistance to fatigue failure is a function of resistance to initiation and/or propagation of microcracks. In a fatigue test, the endurance limit of a bone is the stress level under which no fractures can develop regardless of the number of loading cycles applied. Cortical bone is particularly vulnerable to cyclic stresses. Repeated application of compressive stress can cause progressive accumulation of microcracks. The rate of microcrack accumulation (i.e. microcrack density versus stress cycle number) varies with stress levels. At high stress levels, microdamage initially increases in a non-linear fashion and then stabilizes until just prior to failure. At lower stress levels, initial non-linear crack accumulation occurs, after which damage accumulates rapidly and as a function of applied stress. At a high cycle number, the rate of damage accumulation levels off prior to failure (O'Brien et al. 2005). High stress levels can cause failure at lower microcracks densities than

lower stress ranges. Although cortical bone is relatively susceptible to fatigue failure, repair and remodeling processes provide protection from failure. Microcrack formation plays a role in initiating the remodeling process, based on the hypothesis that disruption of canalicular processes by microcrack formation may be a key trigger (Wang et al. 2016). New bone deposition in the form of secondary osteons arrests microcracks propagation. A balance between stress levels and the rate of remodelling is required for the remodeling process to effectively mitigate fatigue-induced microcracks (Lopez 2019). The most common fatigue fractures reported in Thoroughbred racehorses are fractures of the humerus, tibia, ilium and third metacarpal bone (Martinelli et al. 2003, Ramzan 2011).

The strength of bone is derived from a combination of bone mass (often measured as bone mineral density) and all the other factors that contribute to its strength, also termed bone quality. Bone mineral density can refer to two different measurements:

1) The combined density of a well-defined volume which contains a mixture of both bone and soft tissue, such as a selected volume of medullary trabecular bone in a femur or tibia, is measured as “bone mineral density” (BMD). This parameter relates to the amount of bone within a mixed bone-soft tissue region but does not give information about the material density of the bone itself (Bouxsein et al 2010).

2) The density measurement restricted to within the volume of calcified bone tissue, such as cortical bone, excluding surrounding soft tissue, is called “tissue mineral density” (TMD). By contrast to BMD, TMD gives us information about the material density of the bone itself, and ignores surrounding soft tissue (Bouxsein et al 2010).

Bone quality includes four primary physiologic and structural qualities:

1) rate of bone turnover,

2) bone architecture and geometry,

3) properties of the collagen-mineral matrix,

4) microdamage accumulation.

Bone physiologic and structural qualities are not independent (Burr 2014).

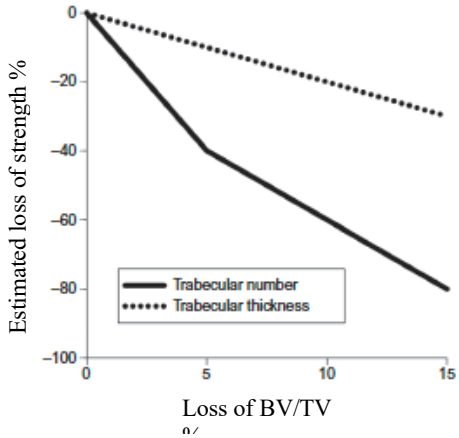

Figure 5: The thickness of the trabecular plates and their number do not contribute equally to the mechanical strength of the structure. A decrease in trabecular number has a much greater negative impact on bone strength than does the loss of an equal amount of bone through trabecular thinning. BV/TV=bone volume fraction, BV=bone volume; TV=trabecular volume. (Burr 2014)

Trabecular bone architecture contributes to the overall cancellous bone volume. The same bone volume can contain trabeculae that are organized in different ways. A connected trabecular architecture (indicated by the C.D.) is important. There is likely to be an ideal relationship between Tb.Th. and Tb.N., dependent on the location and primary direction of loading. However, the loss of complete trabeculae (reducing Tb.N.) reduces the strength and stiffness of bone by two to three times more than does losing the same amount of bone via trabecular thinning (Figure 5). The loss of whole trabeculae reduces connectivity within the entire structure (low C.D.), which makes the structure much less capable of bearing weight

683 and less able to direct stresses to the cortex compared to maintaining the connection but
684 making them thinner (Figure 6) (Burr 2014).
685

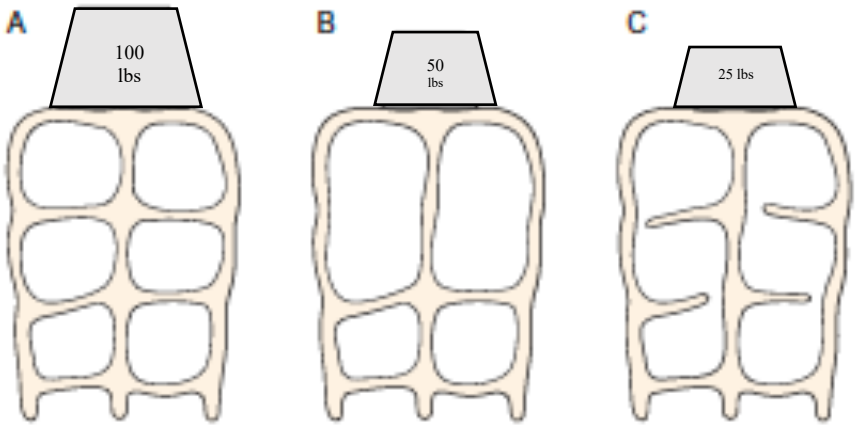

686
687 Figure 6: The importance of bone architecture, independent of the amount of material.
688 Cancellous bone in which the cross struts are disconnected (C) is not very capable of
689 supporting a load, even though there is as much mass as in (A). A smaller mass that is
690 buttressed properly (B) may be able to support more load than a greater mass in which
691 connectivity is compromised.
692

693 Bone's mechanical tensile and compressive strength is also affected by total porosity, another
694 feature of microarchitecture (Augat et al. 2006). Cortical porosity consists of a network of
695 canals which provide conduits for the vasculature to permeate the cortex and, ultimately,
696 sustain the osteocytes. These canals can either be incorporated into the bone during growth
697 as 'primary' canals or can be the products of tissue turnover and thus referred to as
698 'secondary' canals. Secondary canals are associated with secondary osteons. McCalden et al.
699 (1993) reported that cortical porosity explained 76% of the variance in cortical bone ultimate
700 tensile strength. High cortical porosity has been negatively associated with bone elastic

modulus (i.e., material stiffness), toughness, elasticity, and impact energy absorption capacity (Currey 1988).

2.6 Bone adaptation to exercise

Functional adaptation is the response of bone to changes in mechanical demands. The bone response to a given load depends on the strain magnitude and on the interaction of strain magnitude, frequency, rate, distribution and repetitions (Cullen et al. 2001).

In animal loading models, bone adapts within months to new loads showing transient increases in bone formation (modeling) resulting in small regional increases in bone area (Cullen et al. 2000). When load cycle number is extremely high and intense loads are applied, as occurs in military training, an almost pathological response has been measured with up to 11% bone gain in 14 weeks (Margulies et al 1986). More traditional responses to exercise have been reported as a 2.2% increase in tibial BMD after 15 weeks of basic training (Casez et al. 1995) or, in gymnasts, as a 2.8% increase in BMD at the spine after 8 months of training. According to Cullen et al. (2001), as applied force and strain increases, the number of cycles required to initiate bone formation decreases. Short periods of osteogenic cyclical deformation can induce a maximal adaptive response (Boston and Nunamaker 2000, Sinclair et al. 2014).

In the horse, the level of bone deformation increases as a function of locomotor speed (Sinclair et al. 2014). An osteogenic exercise regimen, given for only a short period each day, can rapidly induce a localized adaptive hypertrophy of trabecular bone of the dorsal regions of the third and radial carpal bones, along with a thickening of the subchondral bone plate and a thickening of both the calcified and hyaline layers of the overlying articular cartilage (Firth et al. 1999a,b, Murray et al. 2000). These morphological changes result in a change to the

mechanical properties of the microstructure. Long-term response to loading with associated stiffening of the bone in the dorsal region of the third and radial carpal bones may relate to the common occurrence of cartilage fibrillation and cartilage and subchondral bone breakdown in this region (Sinclair 2014).

If the race-training is based upon a structured increase in duration of short periods of exercise that induces high bone strain, the bone may adapt. The physiologic adaptation (modeling) will condition the bone for athletic exercise. On the other hand, a pathophysiologic response will lead to microdamage and stress-fractures which can lead to catastrophic fractures (Fleck et al. 2003). Accumulation of microcracking within the bone matrix results in a remodeling response in which the secondary bone has long term inferior properties to primary bone. Experimental studies using the non-invasively loaded rat antebrachium have demonstrated that cortical bone in the rat initiates intracortical resorption when the bones are fatigued in vivo (rapid application of osteogenic cyclical loading). Bentolila et al. (1996) demonstrated that intracortical resorption foci occur in association with linear microcracks. By 10 days after cessation of cyclical loading, there are almost 40% fewer linear microcracks present than acutely after fatigue and there is a predominance of secondary osteons (Bentolila 1996). The changes seen in the rat ulna experimental model used by Bentolila et al. (1996), are closely related to those seen in studies on the induction of dorsal third metacarpal disease in Thoroughbred racehorses, using a high volume of high strain rate exercise (Boston and Nunamaker 2000). As mentioned earlier in this chapter, bone remodeling rates are reduced in Thoroughbred racehorses in training, where bone sustains high-magnitude cyclic loading. Remodeling suppression may allow accumulation of microdamage (Jee et al 1990, Jee et al. 1991, Whitton et al. 2010). At sites of high bone density known to be subjected to high loads, such as the third metacarpal bone dorsal cortex and the subchondral bone of the palmar

749 aspect of the third metacarpal condyles, decreased porosity and fewer resorption surfaces are
750 observed when horses are in training compared with those that are resting from training. The
751 association between sclerosis and condylar fractures in racehorses has led to the hypothesis
752 that subchondral sclerosis contributes to fracture formation (Riggs et al. 1999). It was suggest
753 that the marked changes in stiffness at the junction of the sclerotic condyle and the trabecular
754 sagittal ridge result in increased shear forces and, consequently accumulation of microdamage
755 (Riggs et al. 1999). Subsequent focal remodelling increases porosity, which weakens the bone
756 and predisposes to parasagittal condylar fractures. Yet there exists no other evidence for this
757 apart from the observed association (Martig et al. 2014). A detrimental effect of densification
758 is difficult to reconcile with the improved biomechanical properties associated with increased
759 bone volume fraction of metacarpal subchondral bone (Rubio-Martinez et al. 2008, Martig et
760 al. 2014, Martig et al 2020).
761 Controlled osteogenic exercise during training would induce a gradual adaptive response and
762 increase the bone mass with minimal damage of the matrix, thus preserving the mechanical
763 properties of the skeletal structure and reducing the risk of catastrophic failure. Training
764 regimens that appear to optimize bone adaptation without matrix damage comprise short
765 periods of high-intensity exercise (Sinclair 2014, Boston and Nunamaker 2000).
766

767 **2.7 The equine proximal phalanx**

768 **2.7.1 The proximal phalanx as part of the fetlock joint.**

769 The proximal phalanx (PP), together with the third metacarpal/metatarsal bone (MC3) and
770 the proximal sesamoid bones (PSB), form the bone component of the equine
771 metacarpo/metatarsophalangeal joint (fetlock joint) (Figure 7).

The fetlock joint is a high-motion joint that sustains the largest loads of the equine distal limb during locomotion (Merritt et al. 2008, Harrison et al. 2010). A single synovial space is divided into dorsal and palmar/plantar pouches. The dorsal pouch extends approximately 5cm proximal to the joint space, between the third metacarpal bone and the common digital extensor tendon.

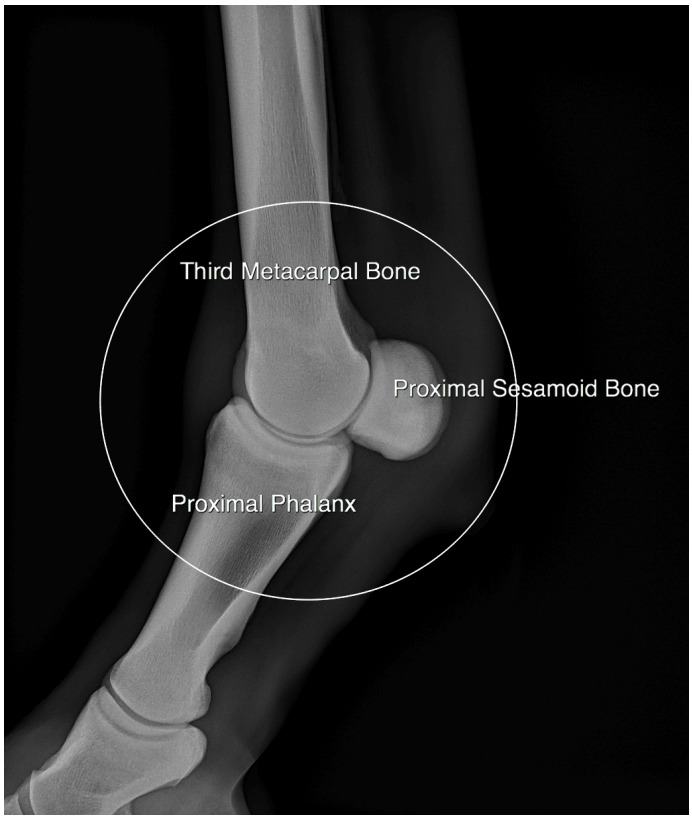

Figure 7: Lateromedial radiographic image of a left fore fetlock joint (metacarpophalangeal joint). The bony components of the joints are indicated.

The palmar/plantar pouch is more voluminous and extends at least 3 cm proximal to the proximal sesamoid bones. The ligamentous elements of the fetlock joint are complex and important. The fetlock joint is supported by an elastic suspensory apparatus composed of the

suspensory ligament, the proximal sesamoid bones and the distal sesamoidean ligaments (Bukowiecki 1987). The suspensory ligament branches insert on the proximal, palmar/plantar abaxial margins of the PSBs and functionally continue through the distal sesamoidean ligaments to attach the distal portion of the PSBs to the proximal and the middle phalanges. From the proximal sesamoid bone insertion, the suspensory ligament branches extend laterally and medially, either side of the fetlock joint, to join the common digital extensor tendon. The suspensory apparatus stores and returns elastic strain energy during locomotion Additional ligamentous support is provided by well-developed medial and lateral collateral metacarpo/metatarsophalangeal and metacarpo/metatarsosesamoidean ligaments, which constrain the almost purely sagittal motion of this joint. The common digital extensor tendon passes over the dorsal aspect of the joint but does not provide any functional support to the joint (Alexander, 1984) (Figure 8).

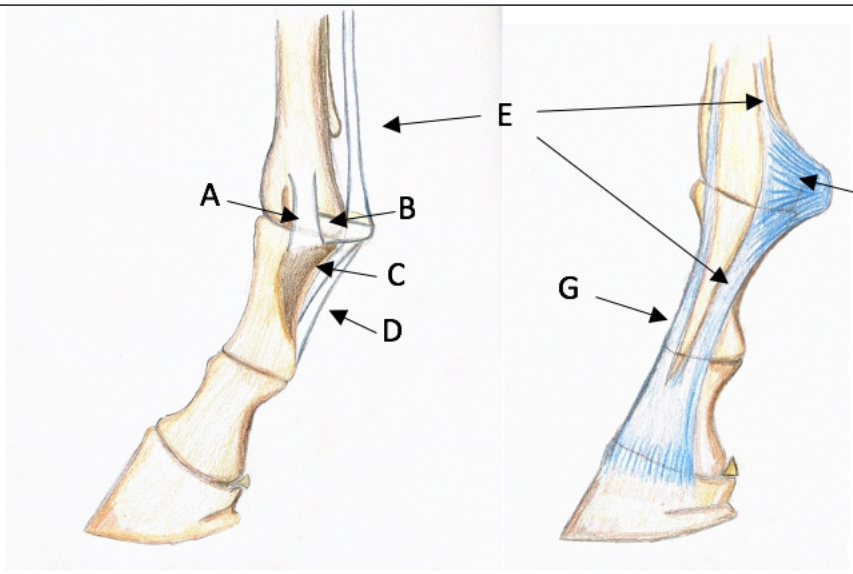

Figure 8: drawing of the ligaments and tendons of the fetlock (A lateral collateral ligament of the fetlock, B lateral collateral ligament of the sesamoid bone, C oblique sesamoid ligament, D straight sesamoid ligament, E suspensory ligament, F palmar annular ligament, G common digital extensor tendon).

2.7.2 Anatomy of the proximal phalanx

The proximal phalanx is a long bone and appears as a cylinder that is flattened on the palmar/plantar aspect and, to a lesser extent, dorsally. The proximal phalanx has well-demarcated cortices, a medullary cavity and a proximal and distal articular surface. On the palmar/plantar aspect, the proximal phalanx presents a triangular rough area for ligamentous insertion of the oblique sesamoidean ligaments. The proximal articular surface of the proximal phalanx is wider than the distal surface, due to narrowing of the bony cylinder at the distal end. The proximal sagittal groove divides the proximal articulating surface into the lateral and medial glenoid cavities and articulates with the sagittal ridge of the distal third metacarpus/metatarsus.

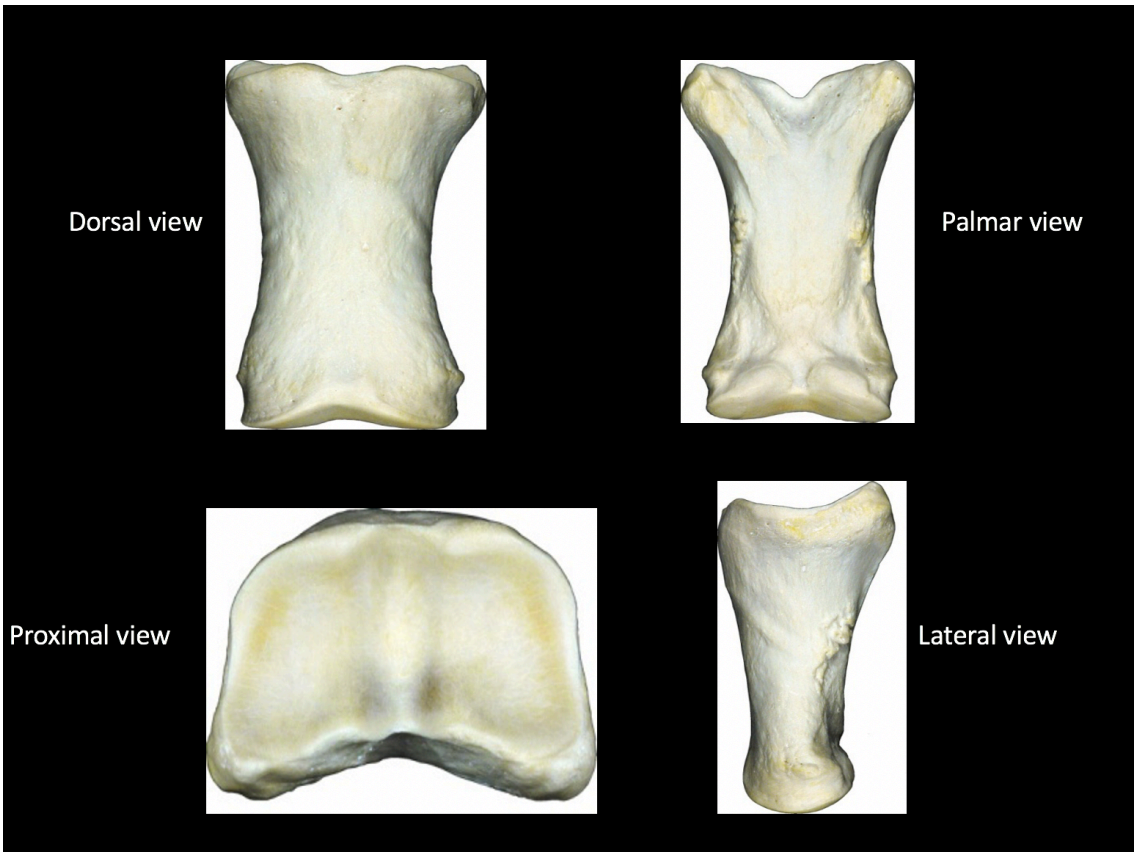

Figure 9: Anatomical images of the dorsal, palmar, proximal and lateral aspects of the equine proximal phalanx (Courtesy of Dr.Sue Stover, DVM, PhD, ACVS)

817 The medial glenoid cavity is slightly wider than the lateral one, matching the anatomy of the
818 congruent distal metacarpal condyles. The distal articular surface of the proximal phalanx is a
819 saddle shaped trochlea, which is congruent with the articular facets on the middle phalanx.
820 The distal articular surface of the proximal phalanx is formed by a lateral and a medial condyle,
821 which are divided by a distal sagittal groove. The medial condyle is slightly larger than the
822 lateral (Parks 2003, Barone 1995) (Figure 9).
823
824 **2.7.3 Biomechanics of the metacarpophalangeal joint**
825 Most of the fetlock joint movements between the MCIII and the PP occur with flexion and
826 extension in the sagittal plane; however, collateromotion (approximately 3°) and axial rotation
827 (approximately 4°) occur (Clayton et al. 2007, Singer et al. 2013). The joint is extended in the
828 normal standing position and hyperextension occurs when high loads are applied, such as in
829 the case of the horse galloping at high speed (Palmer and Bertone 1996). An increase in fetlock
830 joint extension of at least 37° from stance to gallop loads is reported (Singer et al. 2013). In
831 vitro studies showed that movement outside of the sagittal plane is highly correlated with
832 extension of the fetlock joint. In particular, increased collateromotion and external rotation of
833 the PP relative to MCIII is noted as the fetlock joint is subjected to higher loads (Clayton et a.
834 2007, Singer et al. 2013).
835 A finite element analysis model demonstrated that muscle-tendon forces, joint loads and
836 cartilage contact stresses of the MCPJ increase as locomotion speed increases from walking
837 to trotting and finally to cantering (Harrison et al. 2014). I*n vitro,* the contact area of the
838 proximal articulating surface of the PP with the distal condyles of the MCIII is approximately
839 68% when a sagittal plane load of 1,800N, mimicking the stance phase, is applied (Brama et
840 al. 2001). In this condition, the contact area is located slightly towards the palmar/plantar

edge of the joint surface, with a relatively large non-contact area at the dorsal articular margin. When the sagittal plane load is increased to 10,500N, mimicking the gallop, the dorsolateral and dorsomedial joint margins come into full contact. When the load is increased further to 12,000 N, mimicking jumping, the dorsal articular margin comes in full contact, including the sagittal groove (Brama et al. 2001). Joint pressures in the continuously loaded central area of the fetlock joint are relatively low in the standing horse but can increase up to 6-fold when maximum loads are applied. The dorsal articular margin of the PP encounters higher pressures than the central region, but only intermittently during peak loads (Brama et al. 2001). When the fetlock joint loading was investigated during a simulated walk there was a linear increase of the pressure within the sagittal groove of the PP from midstance to break-over, but a decreased pressure on the lateral and medial aspects of the sagittal groove once the mid-stance position had passed, creating a pressure gradient within the proximal articulating surface of the PP (Den Hartog et al. 2009).

2.8 Proximal phalangeal fractures in TB racehorses

2.8.1 Epidemiology

Fractures of the PP are musculoskeletal injuries described both in racehorses (Parkin et al. 2004, Verheyen et al. 2004, Tetens et al. 1997) and in sport horses (Kuemmerle et al. 2008). In racing Thoroughbreds, PP fractures are reported as the first (Bathe 1994) or second (Ramzan et al. 2011) most common long bone fracture, accounting for approximately 15% of all fracture types. PP fractures occur more often during training than during racing (Bathe 1994, Verheyen et al. 2004, Smith 2017), affect fore limbs more than hind limbs (Parkin et al. 2004, Smith 2017) and lack a predilection for left or right limb (Verheyen et al. 2004, Ramzan et al. 2011, Smith 2017). According to Parkin et al. (2004) racing Thoroughbreds competing in

flat races on turf are more commonly affected by PP fractures than racehorses competing on all-weather or in hurdle and steeplechase races. However, epidemiological studies investigating only PP fractures in racing Thoroughbreds are lacking.

2.8.2 Fracture configuration

The most common configuration of PP fractures is sagittal or parasagittal, originating at the proximal articular surface of the sagittal groove and propagating distally (Markel et al 1985, Smith and Wright 2014a). A less commonly reported fracture configuration is the frontal plane longitudinal fracture (Markel et al 1985). A classification for parasagittal fractures of the PP was initially proposed by Markel et al. (1985) and Ellis et al. (1987) and then further revised by Smith and Wright (2014a) as follows:

- Short incomplete: fracture extending in a sagittal plane from the sagittal groove of the proximal articular surface into the epiphysis or metaphysis of the bone, <30 mm distally (Figure 10a).
- Long incomplete: fracture extending in a sagittal plane from the sagittal groove of the proximal articular surface into the diaphysis of the bone, ≥30 mm distally (Figure 10b).
- Complete: fracture extending in a sagittal plane from the sagittal groove of the proximal articular surface into the diaphysis of the bone and exiting into either the proximal interphalangeal joint or through any aspect of the cortex of the bone (Figure 10c).
- Comminuted: complete multipiece (≥3 pieces) fractures of any configuration (Figure 10d).

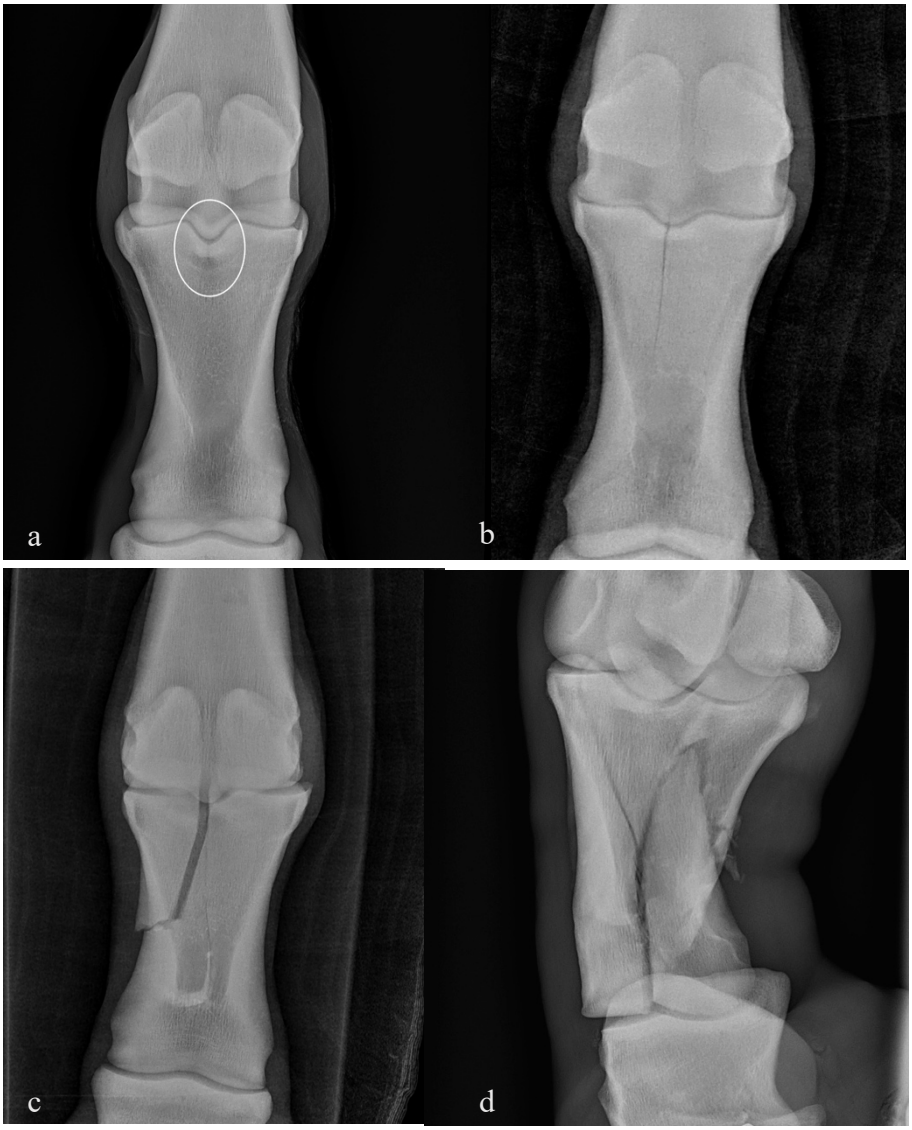

Figure 10: (a) dorsopalmar radiographic image of a short incomplete PP fracture, (b) dorsopalmar radiographic image of a long incomplete PP fracture, (c) dorsopalmar radiographic image of a complete not comminuted PP fracture, (d) dorsolateral-palmaromedial oblique radiographic image of a comminuted PP fracture.

Currently evidence is lacking to determine whether parasagittal fractures originate on the palmar, middle or dorsal aspect of the sagittal groove of the proximal phalanx. In the Thoroughbred racehorse, short incomplete fractures are mainly dorsally located but can also be located midway between the dorsal and palmar/plantar cortices (Richardson and Dyson

914 2011, Ruggles 2011). Brunisholz et al. (2015) found that, in sport horses not used for racing,
915 short incomplete fractures were located more dorsal within the sagittal groove in forelimbs
916 and more plantar in hind limbs.
917
918 **2.8.3 Clinical signs and diagnosis**
919 Clinical signs vary from subtle to obvious lameness and are related to the severity of the
920 fracture. Horses with shorter incomplete parasagittal fractures may show variable degrees of
921 lameness with accompanying signs of fetlock joint effusion, pain on manipulation of the
922 fetlock joint and pain with firm pressure applied over the mid-dorsal aspect of the PP.
923 Complete displaced fractures and comminuted fractures of the PP result in severe non weight-
924 bearing lameness with obvious localizing signs of swelling and pain (Richardson and Dyson
925 2011).
926 Radiography is the imaging modality of choice to diagnose PP fractures; however, short
927 incomplete fractures can sometimes be difficult to visualise with radiography. Magnetic
928 resonance imaging (MRI) and computed tomography (CT) are sensitive techniques for the
929 diagnosis of short incomplete parasagittal fractures of the PP that are not evident on plain
930 radiographs (Nixon 2019, Ruggle 2011, Lipreri et al. 2018). Smith and Wright (2014b) published
931 a retrospective cross-sectional study in which prodromal fracture pathology was detected
932 radiographically in 14% (n=15/110) of the evaluated fractured PPs. The prodromal
933 radiographic changes consisted of irregular periosteal and/or endosteal new bone in the
934 dorsoproximal quadrant of the PP. Moreover, the subchondral bone plate measured at the
935 proximal sagittal groove was significantly thicker in the fractured compared to the
936 contralateral limbs (Smith and Wright 2014b).
937

2.8.4 Management

The main treatment goal for parasagittal fractures of the PP is anatomic reduction, restoration of the articular surface and stabilisation with internal fixation to allow primary bone healing across the fracture site. The choice of treatment is dictated by the fracture configuration, the degree of lameness and concerns about further fracture propagation. Short and long incomplete parasagittal fractures, as well as complete minimally displaced parasagittal fractures are repaired using cortex screws placed in lag fashion. The number of screws is determined by the length and configuration of the fracture. PP fractures without an intact strut of bone are poor candidates for internal fixation. A transfixation cast or an external skeletal fixator device are indicated for salvaging horses with extremely comminuted fractures (Nixon 2019).

2.8.5 Prognosis

Prognosis for return to function of horses that experience PP fractures is determined by multiple factors, including: fracture configuration, extent of proximal articular surface involvement (proximal and distal), treatment chosen and expected athletic career of the horse.

Horses with incomplete fractures of the PP are reported to have a 67- 89% chance to return to racing soundness after treatment (Holcombe et al., 1995). More recently, Smith et al, (2017) reported that 92% of Thoroughbred racehorses with short incomplete parasagittal fractures, managed with internal fixation returned to racing. Prognosis for horses with non-comminuted complete fractures of the PP depends on whether the proximal interphalangeal (PIP) joint is involved. Horses with fractures that enter the PIP joint are reported to have an approximately 50% chance to return to racing. Of those horses with complete fractures that exited the lateral

962 cortex, 71% returned to racing (Holcombe et al., 1995, Markel et al., 1985). Horses with
963 moderately comminuted fractures of the PP have an overall poor prognosis for racing;
964 however, prognosis for survival is good (Kraus et al. 2004). Horses with severely comminuted
965 fractures of the PP have a guarded (58%) prognosis for survival (Kraus et al. 2004).
966
967 **2.8.6 Pathogenesis**
968 The pathogenesis of PP fractures has not been fully elucidated. Debate exists about whether
969 sagittal fractures of the proximal phalanx are the result of an acute monotonic overload or of
970 inadequate adaptive response of the PP subchondral and trabecular bone to exercise.
971 The initial proposed aetiology for parasagittal fractures of the PP related to fetlock joint
972 biomechanics (Rooney 1977). The theory proposed that the fracture occurred during the
973 second half of the stance phase of the stride, as the fetlock joint is moving from an extended
974 to a flexed position. *In vitro* studies showed that an increase in the load (representative of
975 locomotion speed) corresponds to an increased contact between the sagittal ridge of MCIII
976 and the sagittal groove of the PP and, at the same time, to an increased collateromotion and
977 external rotation of PP relative to MCIII (Brama et al. 2001, Den Hartog et al. 2009, Clayton et
978 al. 2007, Singer et al. 2013). Presence of movements outside of the sagittal plane during the
979 phase of maximum load may ultimately lead to fracture as an acute biomechanical event or
980 monotonic overload (Markel & Richardson, 1985; Ellis et al. 1987; Holcombe et al. 1995)
981 In contrast, Fackelman (1973) suggested that parasagittal fractures of the PP are of the fatigue
982 type, as the majority of the musculoskeletal injuries of racehorses, and occur as a result of
983 repeated stress on the bone. The consistent location, the characteristic configuration of
984 parasagittal fractures of the PP and the common presence of reactive periosteal new bone at
985 or adjacent to fracture sites supports this theory (Smith and Wright 2014b). Moreover, all the

horses included in the study sustained a PP fracture during high-speed exercise, and no traumatic event were reported. These characteristics suggest that parasagittal PP fractures are the ultimate manifestation of a more chronic pathological process (Stover and Murray, 2008). A recent study demonstrated that racehorses that experience a parasagittal fracture of the PP have a larger variance of subchondral bone mineral density across the proximal articulating surface of the PP compared to racehorses that did not experience fracture (Noble et al., 2016). Variations of bone mineral density mirror variations in the mechanical properties of bone tissue and may be suggestive of remodelling processes occurring across the proximal aspect of PP (Noble et al., 2016).

2.9 Summary

PP fractures are common orthopaedic injuries of racing Thoroughbreds. As with other musculoskeletal injuries, also proximal phalangeal fractures are a financial and welfare concern. Over the past twenty years, many scientific studies have been investigating the pathogenesis of fractures involving the third metacarpal/metatarsal condyles and the proximal sesamoid bones, however, research investigating PP fractures is lacking. For this reason we decided to focus our attention of fractures of the PP.

Using a finite element analysis, O'Hare et al. (2013) analysed the loads experienced by the PP in stance, walk, trot and gallop. O'Hare's model indicates that the entire sagittal groove experiences high stress when compared with the rest of the bone, supporting the clinical observation that the proximal sagittal groove corresponds to the most common site for fractures in the equine PP. For this reason, we elected to focus our attention on the region of and adjacent to the proximal sagittal groove.

Most studies on fractures of the metacarpal/metatarsal condyles investigate microstructure and biomechanical behaviour of the subchondral bone plate but not of the underlying trabecular bone. However, Toth et al. (2013) found a linear correlation between the trabecular bone region bone mineral density and fatigue strength. Multiple clinical studies recognized osseous trauma within both the subchondral bone and the adjacent trabecular bone of the proximal sagittal groove of the PP as a cause of lameness in Thoroughbred racehorses and sports horses. This osseous trauma is usually detected with advanced imaging modalities, such as MRI and gamma scintigraphy (Dyson et al. 2011, Ramzan et al. 2010, Gold et al. 2017, Lipreri et al. 2018). It was speculated that osseous trauma detected withing the SCB and TBB of the proximal sagittal groove may represent early stage of PP fracture (Ramzan et al. 2010). As a result, we elected to investigate not only the subchondral bone but also the trabecular bone within the region of the proximal sagittal groove.

The aim of this study was to analyse the microstructural and anisotropic characteristics of the subchondral (SCB) and trabecular (TB) bone of the proximal sagittal groove of the PP in horses with different training history (racing and non-racing) and injury status (with and without a proximal phalangeal fractures) using micro-computed tomography (μCT) with the following objectives:

1) To understand the effect of race-training on the microstructural characteristics of the SCB and TB of the proximal sagittal groove of the PP.

2) To understand the potential contribution of inadequate adaptive bone response of SCB and TB to the pathophysiology of PP fractures in race-trained horses

3) To use the information from Objectives 1 and 2 to help identify clinical strategies to identify horses at increased risk of fracture of the PP.

We hypothesised that:

1) Microstructural characteristics of the subchondral and trabecular bone of the proximal sagittal groove of the PP would vary significantly across the dorso-to-palmar and medial-to-lateral aspects of the proximal sagittal groove of race-trained horses that have sustained a PP fracture.

2) Microstructural characteristics of the subchondral and trabecular bone of the proximal sagittal groove of the PP would vary significantly between race-trained and untrained horses. We expect an overall increase in bone density (BMD and BV/TV), decreased total porosity and increased trabecular thickness in race-trained horses compared to untrained horses.

3) Microstructural characteristics of the subchondral and trabecular bone of the proximal sagittal groove of the PP would vary significantly between race-trained horses that had not sustained PP fracture and race-trained horses that had sustained PP fracture. In particular, we expect evidence of disruption of trabecular architecture (low trabecular number, low connectivity density and low degree of anisotropy) in horses that experience a PP fracture.

Chapter 3

Materials and Methods

3.1 Ethical approval

Ethical approval for the study was granted by the University of Liverpool Veterinary Research Ethics Committee (VREC507). About 70 % of the samples for the study were collected from material previously saved from approved projects carried out with Horserace Betting Levy Board (HBLB) funding. The rest of the samples were collected from horses euthanized at the University of Liverpool for reasons unrelated to the project or from horses referred to the University of Liverpool for post-mortem investigation. The study is a cadaver study and relies on post-mortem dissection only.

3.2 Sample population

The proximal phalangeal bones were collected post-mortem from three groups of horses:

A. Untrained Control Group (UC): Bones in this group were from horses that had never undergone race-training and that were euthanized for reasons other than limb fracture.

B. Race-Trained Control Group (TC): Bones from race-fit Thoroughbreds that were euthanized for reasons unrelated to musculoskeletal injury. The left or right fore PP was randomly selected for collection.

C. Race-Trained Fractured Group (TF): Bones from race-fit Thoroughbreds that were euthanized having sustained a comminuted fracture of the PP. The contralateral non-fractured PP to a fractured PP was collected.

3.3 Sample processing for microcomputed tomography (μCT) imaging

Following disarticulation from the metacarpophalangeal and proximal interphalangeal joint, the PPs were cleaned of surrounding soft tissue, wrapped in wet paper towel and cling film

and stored frozen at -20° until further sectioning. Before sectioning, the bones were defrosted at room temperature over a 24-hour period.

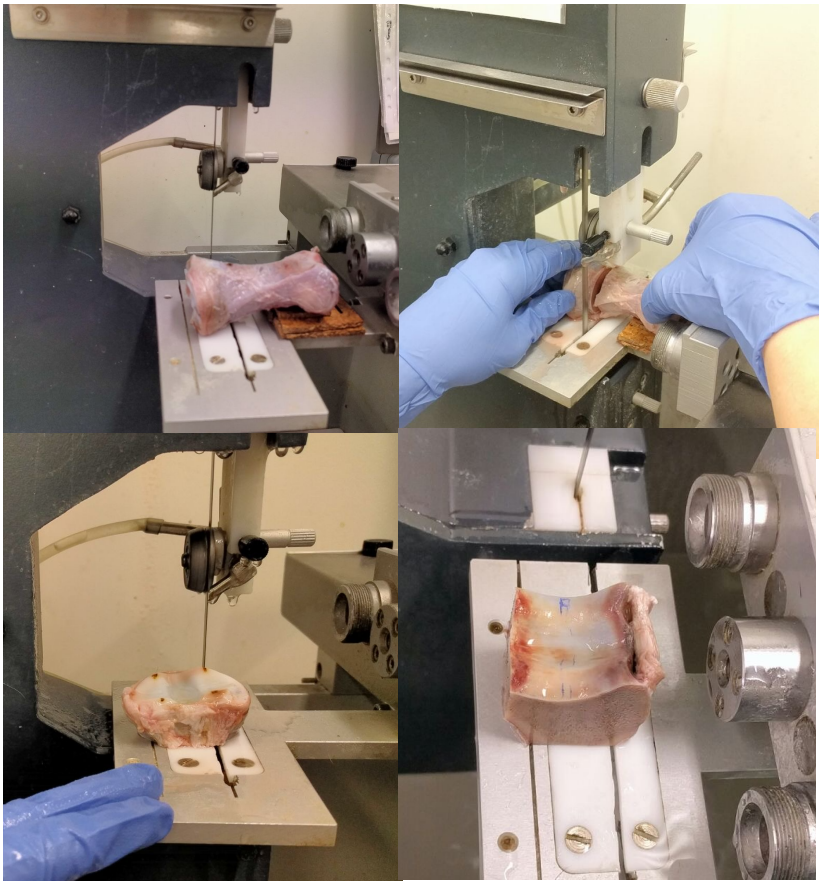

Figure 11: images showing how the bone blocks are obtained using a Diamond Band Pathology Saw (Exakt Technologies Inc.)

Once defrosted, the bones were initially sectioned transversally, 2 cm distal to the sagittal groove using a Diamond Band Pathology Saw (Exakt Technologies Inc.). Two parasagittal cuts were then made 1 cm lateral and 1 cm medial to the most distal point of the sagittal groove (Figure 11). An approximately 2 mm section of the palmar aspect of the bone was removed in order to obtain a flat surface. The dimensions of the sample were determined by the maximum size that fit the sample chamber of the micro-computed tomography (µCT) scanner

(Skyscan1272, Bruker, Belgium). The blocks of bone were fixed in a 10% formalin solution for 72 hours and then stored in 70% ethanol until µCT was performed.

3.4 Acquisition of microCT images

Shortly before µCT imaging, the bone samples were removed from 70% ethanol solution and the outside was dried using tissue paper. The sample was then tightly wrapped with paraffin film (Laboratory Parafilm®) to prevent drying of the bone sample. The sample was then positioned on a support in vertical position, with the palmar aspect of the sample facing down. The sample was secured to the support using dental wax. The samples were then placed into the µCT scanner (Skyscan1272, Bruker, Belgium) and the microtomographic images acquired (Figure 12). The following settings were selected:

- Rotation: 0.4° stepsize over 180°
- Energy filter: Al 1mm
- Pixel size: 15 µm
- IBinning: 3x3, resulting in 1344x896 pixel X-Ray projection images
- Offset scan with two camera positions
- X-ray source: 70kV and 142µA.
- Exposure time: 2596ms
- Volumetric reconstruction of the acquired images was performed using NRecon® reconstruction software (Output scaling to 8-bit: 0-0.07, Ring artefact correction 5, Beam hardening correction 38%).

After image reconstruction, the µCT attenuation values were calibrated into hydroxyapatite density (mg/cm^3) by use of a hydroxy-apatite calibration phantom (QRM GmbH MicroCT-HA Phantom, Diameter=25mm, Inserts=5mm diameter, HA 0, 50, 200, 800, 1200 mg/cm^3).

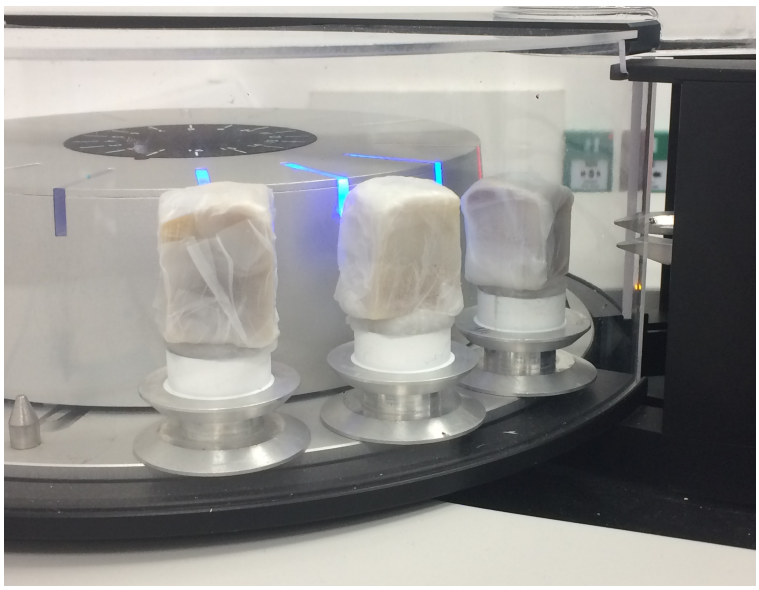

Figure 12: Image showing the bone blocks into the µCT scanner. The bone blocks are tightly wrapped with paraffin film (Laboratory Parafilm®) and positioned on a support in vertical position

3.5 MicroCT image analysis

Following volumetric reconstruction of the acquired images (Figure 13), a total of 18 volumes of interest (VOIs) were defined using Dataviewer software (Bruker Skyscan, Belgium) (Figure 14). Nine volumes of interest (VOIs) were identified within the SCB layer and 9 within the TBB layer. Each volume of interest was saved as a separate dataset using Dataviewer. The VOIs within the subchondral bone measured 1500mm x 1500mm x 1500mm and the VOIs within the trabecular bone measured 5250mm x 5250mm x 5250mm. The VOIs within the trabecular layer were positioned 3750mm distally to the VOIs within the subchondral bone layer. In each layer, the VOIs were localized at 25% (dorsal), 50% (middle) and 75% (palmar) of the distance from dorsal to palmar as measured across the articular surface of the PP. Within these three regions, the VOIs were classified as central (halfway between the lateral and medial aspect of

the sagittal groove), medial (7 mm medial to the central region of the sagittal groove) and lateral (7 mm lateral to the central region of the sagittal groove) (Figure 14).

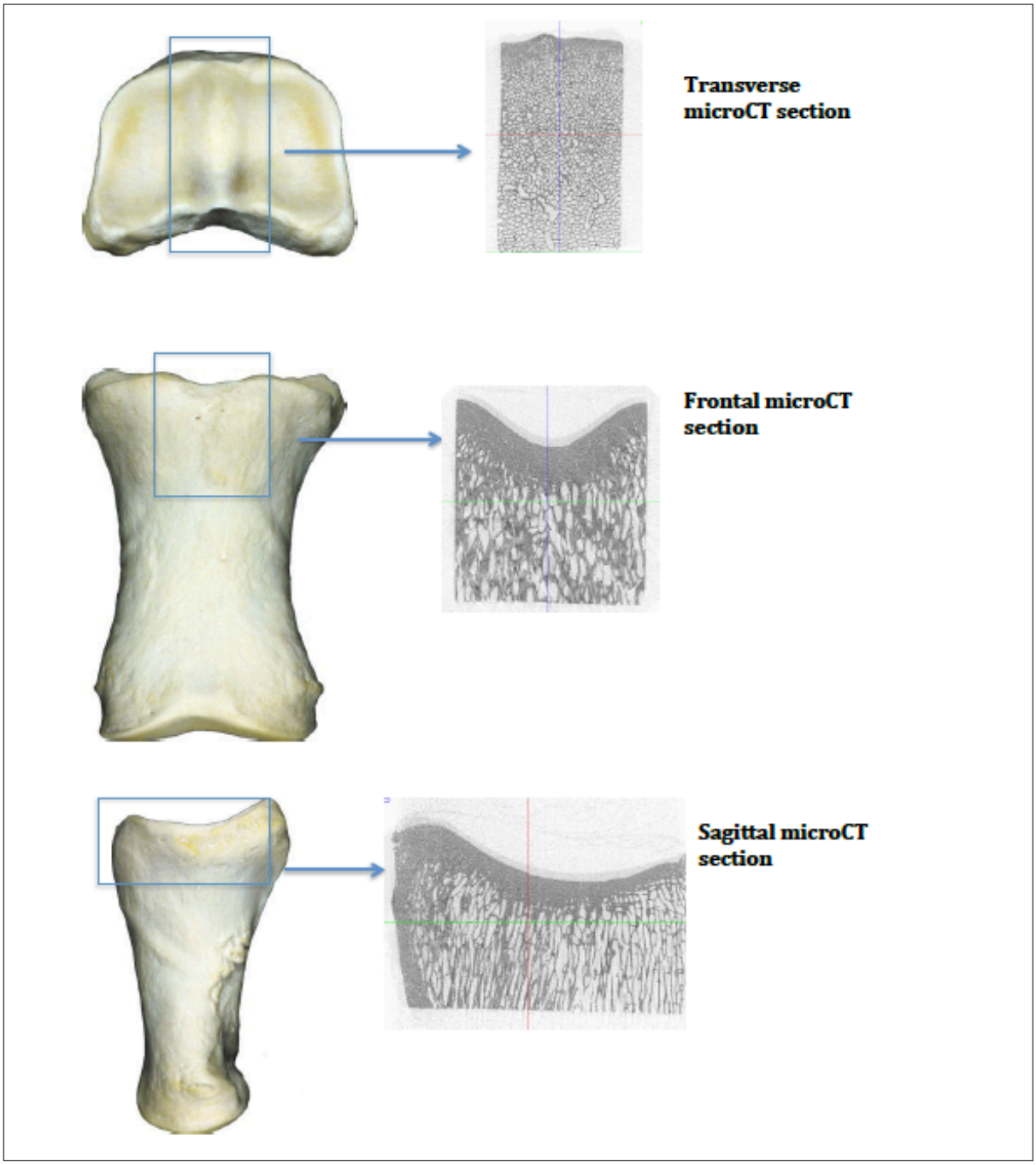

Figure 13: schematic representation a transverse, frontal and sagittal µCT section following volumetric reconstructions of the acquire images

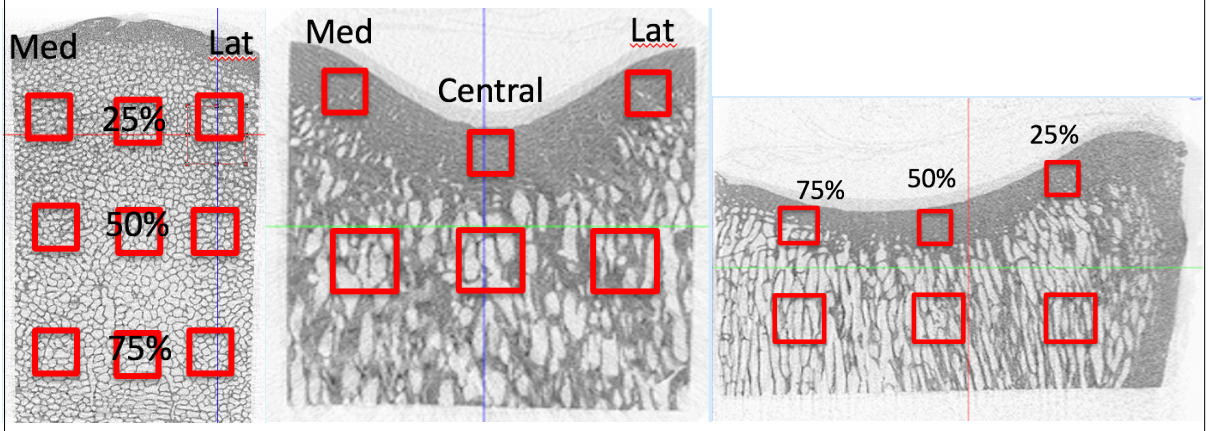

Transverse section Frontal section Sagittal section

Figure 14: schematic representation of the 18 VOIs identified within the subchondral and trabecular bone of the proximal sagittal groove of the PP. Both within the subchondral and the trabecular bone , the VOIs were localized at 25% (dorsal), 50% (middle) and 75% (palmar) of the distance from dorsal to palmar as measured across the articular surface of the PP. Within the dorsal, middle and palmar regions, the VOIs were classified as central (halfway between the lateral and medial aspect of the sagittal groove), medial (7 mm medial to the central region of the sagittal groove) and lateral (7 mm lateral to the central region of the sagittal groove).

Each VOI was analysed using a µCT bone analysis software (CTAn, Bruker Skyscan, Belgium). Tissue mineral density (TMD mg/cm^3 - density restricted to the calcified bone tissue, excluding surrounding soft tissue), was calculated for each VOI within both the subchondral bone and the trabecular bone layer. Total porosity was calculated for VOIs within the subchondral bone only. Bone volume fraction (BV/TV – proportion of total volume of the cube of bone that was occupied by bone tissue), trabecular thickness (Tb.Th µm), trabecular separation (Tb.Sp µm), trabecular number (Tb.N. 1/µm), connectivity density (C.D. - number of trabecular connections/µm^3), and degree of anisotropy (D.A. measure of how highly oriented substructures are within a volume) were calculated for each VOI within the trabecular bone layer only. The parameters were software generated (CTAn, Bruker Skyscan, Belgium).

3.6 Statistical analysis

Statistical analysis was performed using GraphPad Prism®. Data were assessed for normality using Shapiro-Wilk test. ANOVA and Friedman's test were used respectively for normally and non-normally distributed data to investigate how the parameters varied between VOIs within each group and how the three experimental groups differed from each other.

Statistical analysis within each group. Separately within the lateral, central and medial aspect of the subchondral bone layer of the sagittal groove, each variable was compared between dorsal (25%), middle (50%) and palmar (75%). Moreover, separately within the dorsal (25%), middle (50%) and palmar (75%) aspect of the subchondral bone layer of the sagittal groove, each variable was compared between the lateral, central and medial aspects of the sagittal groove. The same comparisons were then performed within the trabecular bone layer of the sagittal groove.

Statistical analysis between groups. The variables measured in each of the 18 VOIs were compared between the three groups.

Statistical significance was set with a P value <0.05. However statistical results with a P value between 0.05 and 0.1 were kept in consideration. These results with a P value higher than 0.05 but less or equal to 0.1, even if not statistically significant, were interpreted as indicators of "trends".

Chapter 4

Results

4.1 Sample population

Proximal phalanges were collected from 23 horses and were assigned to three experimental groups: untrained control (UC; n=6), race-trained control (TC; n=9) and race-trained fracture (TF; n=8). The untrained control group consisted of 4 geldings and 2 mares. Their mean age was 10.8 years (range 3-10 years). Three PPs were from the left front limb and 3 from the right front. Horses included in the race-trained control group were all geldings with a mean age of 8.4 years (range: 5-10 years). Seven were competing in National Hunt races and two in flat races. Five PPs were from the left front limb and 4 from the right front limb. The race-trained fracture group consisted of seven geldings and one colt. Their mean age was 7.25 years (range 5-11 years). One horse was competing in flat races and the other seven were competing in National Hunt races. Five PPs were from the left front limb and 3 from the right front. The fractures had a comminuted configuration. PPs from hind limbs were not included.

	UC	**TC**	**TF**
Number	n=6	n=9	n=8
Gender	n=2M, n=4G	n=9G	n=7G, n=2C
Age	range 3-10 years	range: 5-10 years	range 5-11 years
Limb	3LF, 3RF	5LF, 4RF	5LF, 3RF
Discipline	Low level riding	7NH, 2F	7NH, 1F

Table 1: summary of the sample population details. M= mare, G= gelding, C=colt, LF= left fore limb, RF= right fore limb, NH= national hunt races, F= flat races

4.2 Subchondral bone

4.2.1 Tissue Mineral Density

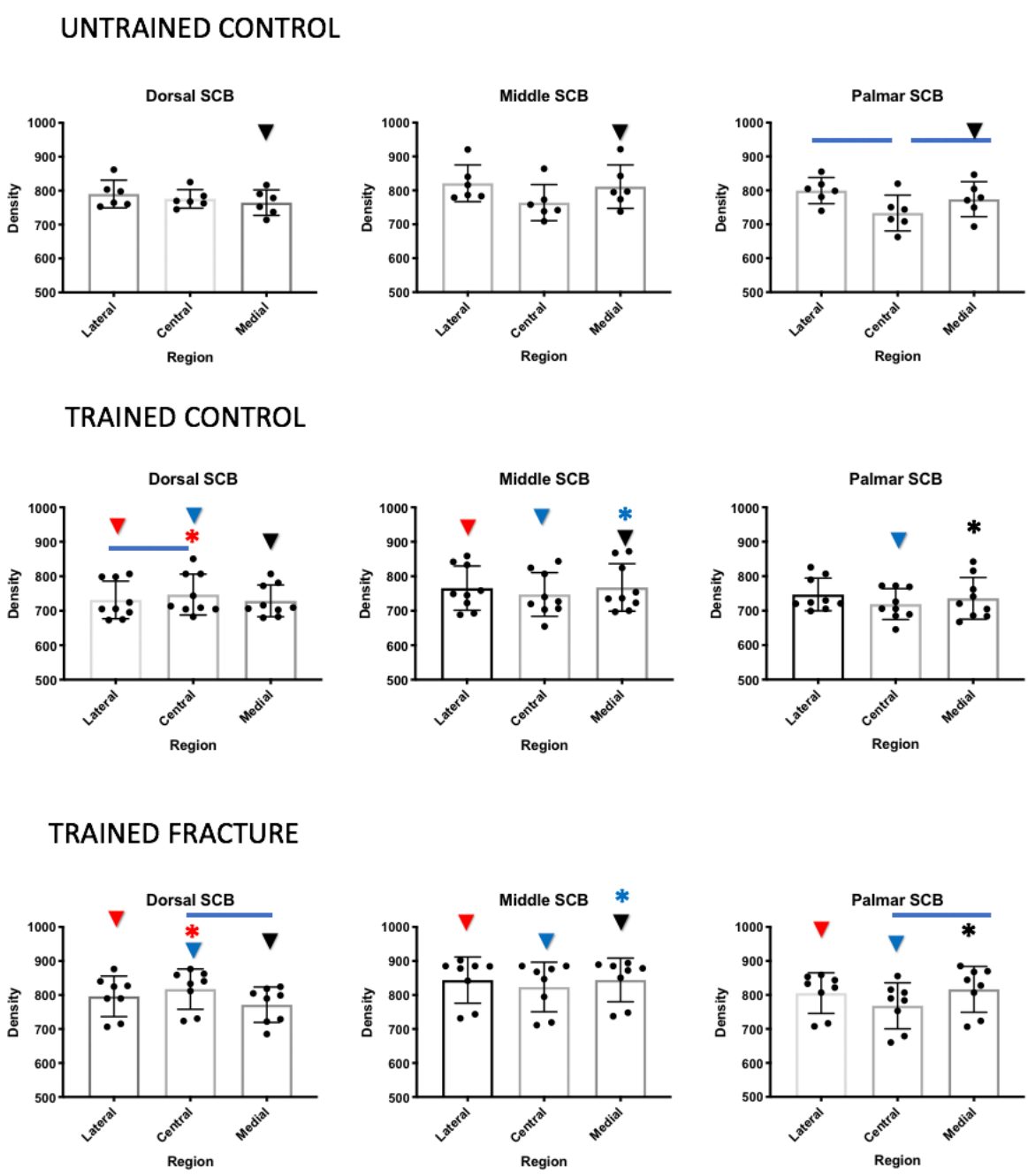

Figure 15: Scatter plots illustrating the subchondral bone (SCB) Tissue Mineral Density (TMD) results. The significant difference in SCB TMD from the lateral to medial aspects, within groups, is reported with a blue bar above the columns. The significant difference in SCB TMD from the dorsal to palmar aspect, within groups, is reported with a down-pointing triangle (▼). Red= lateral; Blue = central; Black = medial. The significant difference in SCB density between the 3 groups is indicated by an asterisk (*). Red= dorsal; Blue= middle; Black = palmar.

WITHIN GROUPS

When assessed in a frontal plane (lateral to medial), the subchondral bone tissue mineral density (SCB TMD) of the UC group is similar from lateral to medial in the dorsal and middle aspects of the sagittal groove. However, in the palmar aspect of the sagittal groove, the SCB TMD is lower in the central region compared to the lateral (p=0.0007) and medial (p=0.006) regions. In both race-trained groups (TC, TF), the SCB TMD in the dorsal aspect of the sagittal groove is higher in the central region compared to the adjacent lateral (TC, p= 0.04) and medial (TF, p= 0.003) regions.

When assessed in sagittal plane (from dorsal to palmar), the SCB TMD of the UC group is similar in the lateral and central aspects. However, within the medial aspect, the SCB TMD is higher in the middle region compared to the dorsal (p=0.04) and palmar (p=0.02) regions. A similar pattern is noted also in the medial aspect of the sagittal groove of race-trained horses (TC and TF), where the SCB TMD is higher in the middle region compared to the dorsal region (TC, p=0.006, TF, p= 0.0009).

BETWEEN GROUPS

There were no significant differences in SCB TMD of the sagittal groove between the UC group and both race-trained groups (TC and TF). However, the SCB TMD of the TC group was significantly lower centrally in the dorsal aspect (p=0.03), and medially in the palmar aspect (p=0.04) of the sagittal groove compared to the TF group. Moreover, in the TC group, the SCB TMD of the lateral aspect of the sagittal groove was lower in the dorsal (p=0.09), middle (p=0.06), and palmar (p=0.07) aspects compared to the TF group.

SCB VOI	UC		TC		TF	
	Mean	SD	Mean	SD	Mean	SD
VOI 1	696.52	19.7261289	767.26	70.1667817	790.09	40.8652216
VOI 2	709.71	19.7479687	776.56	70.918473	775.85	27.4500206
VOI 3	699.52	14.7500174	754.25	59.8491696	764.92	37.4942592
VOI 4	726.15	29.9672099	807.52	82.4260375	820.91	54.1994089
VOI 5	708.57	29.5237587	768.65	79.9932106	764.05	24.2743477
VOI 6	710.99	22.2624118	811.09	75.8478237	811.22	26.8604497
VOI 7	700.94	24.6092161	770.33	82.953746	782.99	37.1738235
VOI 8	692.9	27.3511088	731.47	79.9305848	733.39	52.5667895
VOI 9	713.3	35.293822	779.25	75.8342339	774.03	51.510182

Table 2 – Means and standard deviations for subchondral bone Tissue Mineral Density (SCB TMD, units of mg/cm^3

4.2.2 Total Porosity

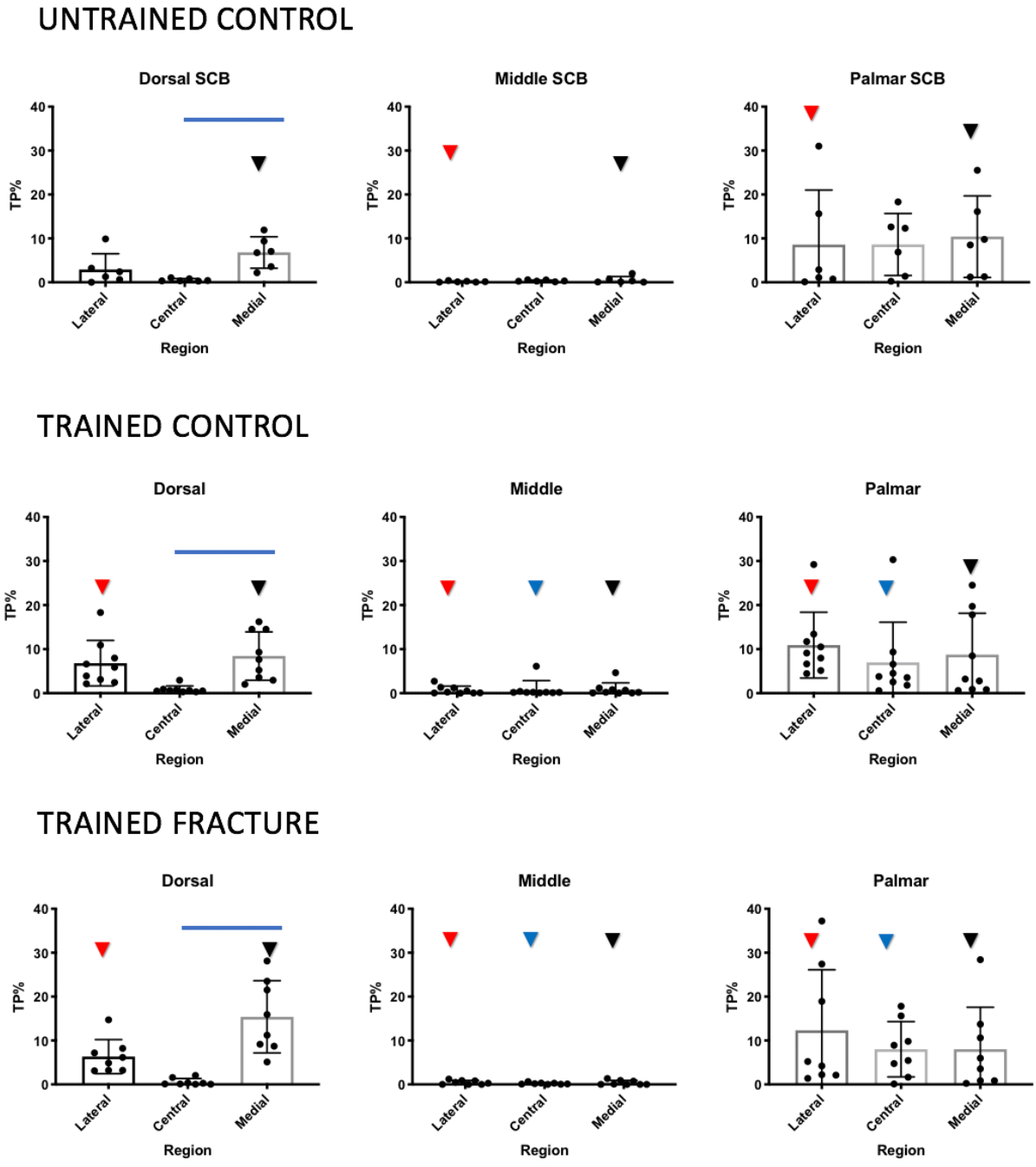

Figure 16: Scatter plots showing the subchondral bone (SCB) Total Porosity (TP) results. The significant difference in SCB TP from the lateral to medial aspects, within groups, is reported with a blue bar above the columns. The significant difference in SCB TP from the dorsal to palmar aspect, within groups, is reported with a down-pointing triangle (▼). Red= lateral; Blue = central; Black = medial. The significant difference in SCB TP between the 3 groups is indicated by an asterisk (*). Red= dorsal; Blue= middle; Black = palmar. There are no significant differences in SCB TP between the three groups.

WITHIN GROUPS

When assessed in a frontal from plane, the subchondral bone total porosity (SCB TP) was significantly lower in the central region compared to the medial region in the dorsal aspect of all three groups (UC p=0.002, TC p=0.002, TF p=0.0005). When assessed in a sagittal plane, in the UC group, the SCB TP is significantly lower in the middle compared to the palmar locations (p=0.02) on the lateral aspect of the sagittal groove. In the medial aspect, the SCB TP is significantly lower in the middle compared to both the dorsal and palmar aspects (p=0.02). In the central aspect of the groove, the SCB TP tends to be lower in the middle compared to the palmar region (p=0.1). The patterns described above for UC are similar in the TC and TF groups with the addition of significant differences laterally between dorsal and middle (p=0.02) and middle and palmar (p=0.006), and centrally between middle and palmar (p=0.0005). The pattern was similar between the bones of the two race-trained groups.

BETWEEN GROUPS

There are no significant differences in subchondral bone total porosity between the three groups. However, in the dorso-lateral and dorso-medial aspect of the sagittal groove, the SCB TP tends to be higher in the TF group compared to the UC group (p=0.1).

SCB VOI	UC		TC		TF	
	Mean	SD	Mean	SD	Mean	SD
VOI 1	2.91E+00	3.60696243	6.82E+00	5.17482239	5.96E+00	3.80281684
VOI 2	5.43E-01	0.31227984	8.36E-01	0.81544263	5.81E-01	0.73175295
VOI 3	6.81E+00	3.60787752	8.44E+00	5.48885081	1.38E+01	9.01727088
VOI 4	1.66E-01	0.13590184	6.96E-01	0.92027236	4.20E-01	0.44930351
VOI 5	3.48E-01	0.18343023	8.58E-01	1.97923483	2.37E-01	0.20515846
VOI 6	5.54E-01	0.75503557	8.75E-01	1.47261566	3.71E-01	0.50055455
VOI 7	8.57E+00	12.4459378	1.09E+01	7.45457162	1.12E+01	13.3067181
VOI 8	8.62E+00	7.05761944	7.00E+00	9.12202845	7.19E+00	6.37414197
VOI 9	1.04E+01	9.27043514	8.75E+00	9.40054242	7.23E+00	9.26254666

1334 Table 3 – Means and standard deviations for subchondral bone Total Porosity (SCB TP %)
1335

4.3 Trabecular Bone

4.3.1 Tissue Mineral Density

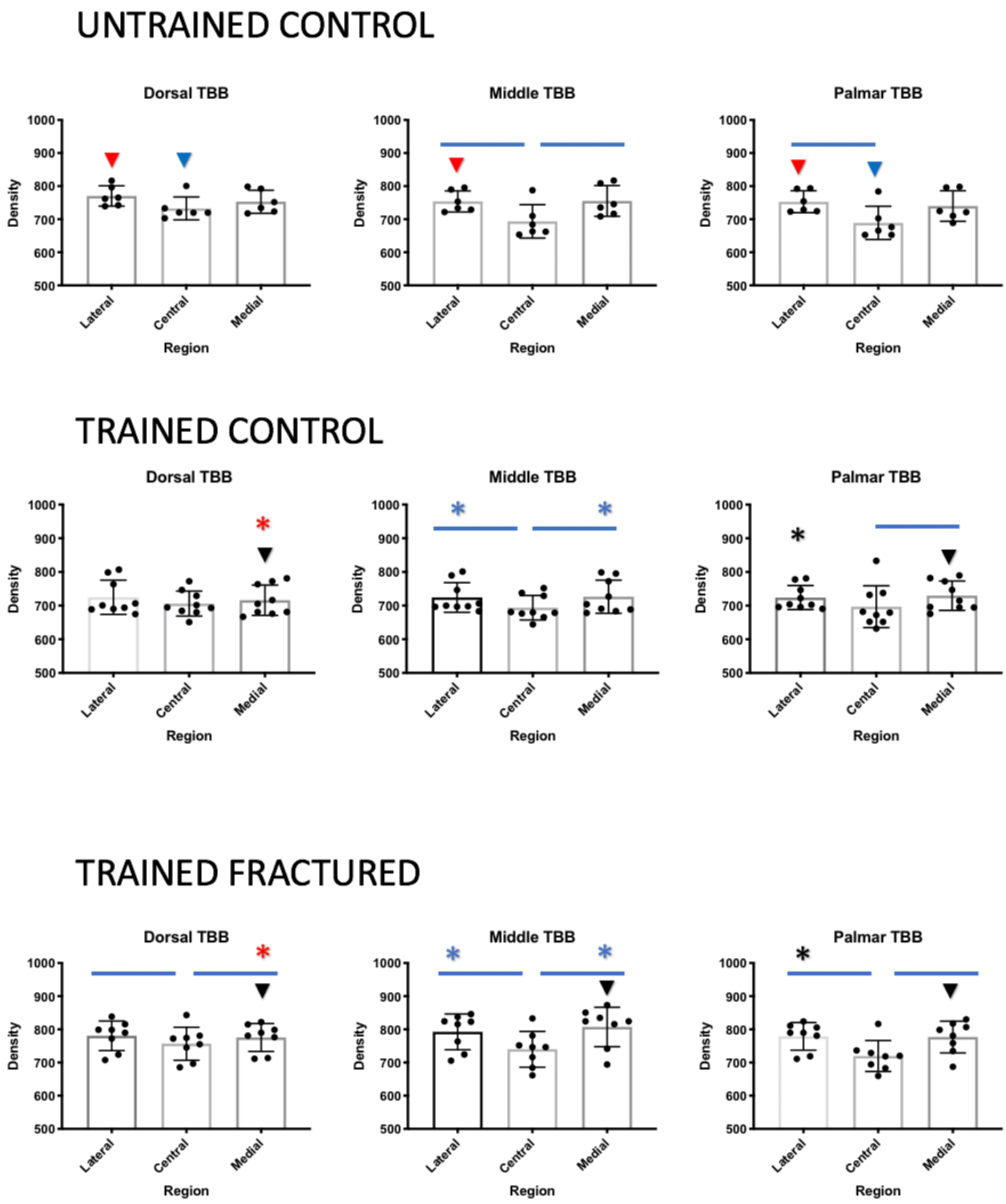

Figure 17: Scatter plots with bar showing the trabecular bone (TbB) Tissue Mineral Density (TMD) results. The significant difference in TbB TMD from the lateral to medial aspects, within groups, is reported with a blue bar above the columns. The significant difference in TbB TMD from the dorsal to palmar aspect, within groups, is reported with a down-pointing triangle (▼). Red= lateral; Blue = central; Black = medial. The significant difference in TbB TMD between the 3 groups is indicated by an asterisk (*). Red= dorsal; Blue= middle; Black = palmar.

WITHIN GROUPS

When assessed on a frontal plane, the trabecular bone TMD (TbB TMD) of the lateral (UC p=0.02, TC p=0.002, TF p=0.02) and medial (UC p=0.02, TC p=0.006, TF p=0.002) aspects of the middle region is significantly higher compared to the central aspect in all three groups. In the palmar region, the TbB TMD of only the lateral aspect is significantly higher than the central aspect (p=0.01) in the UC group, with only the medial aspect higher in the TC group (P= 0.02). However, in the TF group, the TbB TMD of both the dorsal and palmar aspects was significantly higher laterally (dorsal p=0.03, palmar p=0.001) and medially (dorsal p=0.04, palmar p=0.003) compared to the central region.

When assessed on a sagittal plane, in the UC group, TbB TMD in the dorsolateral aspect of the sagittal groove is significantly higher than in the middlelateral (p=0.0007) and palmarolateral (p=0.0007) aspects. In the central region, the TbB TMD is significantly higher in the dorsal region compared to the palmar region (p=0.01). The pattern was different in the race-trained groups. In the TC group, the TbB TMD in the palmaromedial aspect of the sagittal groove is significantly higher than in the dorsomedial aspect (p=0.04). In the TF group, the TbB TMD in the middle-medial aspect of the sagittal groove is significantly higher than in the dorsomedial (p=0.03) and palmaromedial (p=0.006) aspects.

BETWEEN GROUPS

No significant differences are noted between the UC and the TC group or between the UC and the TF groups. However, the TbB TMD was significantly higher in the TF group compared to the TC group in the dorsomedial (p=0.02) middle-medial (0.008), middle-lateral (p=0.01) and palmarolateral (p=0.01) regions.

TBB VOI	UC		TC		TF	
	Mean	SD	Mean	SD	Mean	SD
VOI 10	692.46	10.9712816	767.94	56.35857	770.33	30.5141803
VOI 11	684.22	18.0108201	736.47	64.8862018	732.8	34.6360191
VOI 12	687.74	19.0016209	757.95	52.9979702	753.01	34.8954634
VOI 13	696.74	7.64535522	778.12	63.798551	753.89	31.8768356
VOI 14	671.07	14.1536433	714.35	70.5912489	693.45	50.5074715
VOI 15	695.34	17.7442845	778.9	72.3691709	755.28	46.469362
VOI 16	701.96	11.1727998	767.59	51.2672748	752.72	33.1271439
VOI 17	661.58	19.5567296	709.82	62.7065169	689.09	50.0817146
VOI 18	703.74	24.4080237	759.44	55.1661144	739.94	45.9506849

Table 4 – Means and standard deviations for trabecular bone Tissue Mineral Density (TbB TMD, units of mg/cm^3)

4.3.2 Bone Volume Fraction

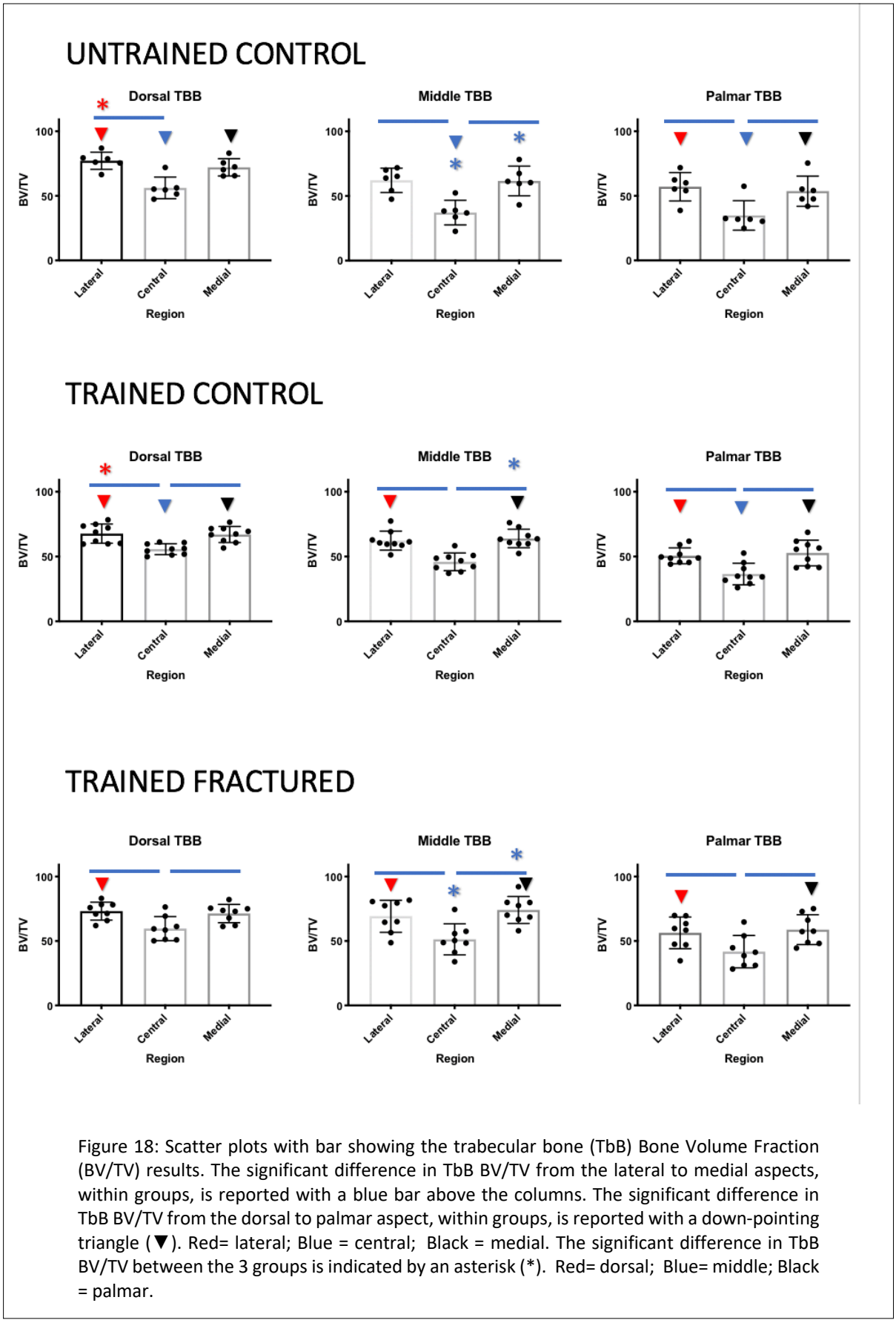

Figure 18: Scatter plots with bar showing the trabecular bone (TbB) Bone Volume Fraction (BV/TV) results. The significant difference in TbB BV/TV from the lateral to medial aspects, within groups, is reported with a blue bar above the columns. The significant difference in TbB BV/TV from the dorsal to palmar aspect, within groups, is reported with a down-pointing triangle (▼). Red= lateral; Blue = central; Black = medial. The significant difference in TbB BV/TV between the 3 groups is indicated by an asterisk (*). Red= dorsal; Blue= middle; Black = palmar.

WITHIN GROUPS

When assessed in a frontal plane, in the UC group, the TbB BV/TV within the lateral aspect was higher compared to the central aspect in the dorsal ($p=0.001$), middle ($p=0.001$) and palmar regions ($p=0.001$). In the TC and TF groups, the TbB BV/TV within the lateral and medial aspects was higher compared to the central aspect in the dorsal (TC lateral $p=0.002$, TC medial $p=0.006$, TF lateral $p=0.001$, TF medial $p=0.03$), middle (TC lateral $p<0.0001$, TC medial $p<0.0001$, TF lateral $p=0.01$, TF medial $p=0.003$), and palmar regions (TC lateral $p=0.001$, TC medial $p=0.009$, TF lateral $p=0.01$, TF medial $p=0.003$).

When assessed in a sagittal plane, in the UC group, the TbB BV/TV is significantly higher dorsally than palmarly in the lateral ($p=0.002$), central ($p<0.0001$) and medial ($p=0.01$) aspects. Moreover, in the central aspect, the TbB BV/TV is significantly higher in the dorsal compared to the middle region ($p=0.008$). A similar trend is also noted in the race-trained groups, where the TbB BV/TV decreases from dorsal to palmar.

BETWEEN GROUPS

The TbB BV/TV in the dorsolateral region is significantly higher in the UC group than in the TC group ($p=0.04$). However, in the middlecentral region, the TbB BV/TV is significantly lower in the UC group compared to the TF group ($p=0.03$). In the middlemedial aspect of the sagittal groove, the TbB BV/TV tends to be lower in the UC ($p=0.06$) and TC group ($p=0.09$) compared to the TF group.

TBB VOI	UC		TC		TF	
	Mean	SD	Mean	SD	Mean	SD
VOI 10	7.72E+01	6.62891458	6.77E+01	7.36967437	7.36E+01	6.63871154
VOI 11	5.62E+01	8.37886163	5.57E+01	4.23E+00	5.92E+01	8.86357019
VOI 12	7.21E+01	6.69011709	6.70E+01	6.17699214	7.19E+01	6.87405459
VOI 13	6.21E+01	9.44922143	6.23E+01	7.30688649	6.94E+01	11.6078756
VOI 14	3.72E+01	9.56549745	4.59E+01	6.80809714	4.95E+01	12.4841196
VOI 15	6.16E+01	11.4422525	6.39E+01	7.15863226	7.36E+01	9.93785896
VOI 16	5.70E+01	11.0026849	5.06E+01	6.13708432	5.73E+01	11.862956
VOI 17	3.48E+01	11.4027251	3.66E+01	8.34157753	4.11E+01	11.938421
VOI 18	5.36E+01	11.7384382	5.28E+01	9.87909945	5.94E+01	10.9834282

Table 5 – Means and standard deviations for trabecular bone Bone Volume Fraction (TbB BV/TV %)

4.3.3 Trabecular Thickness

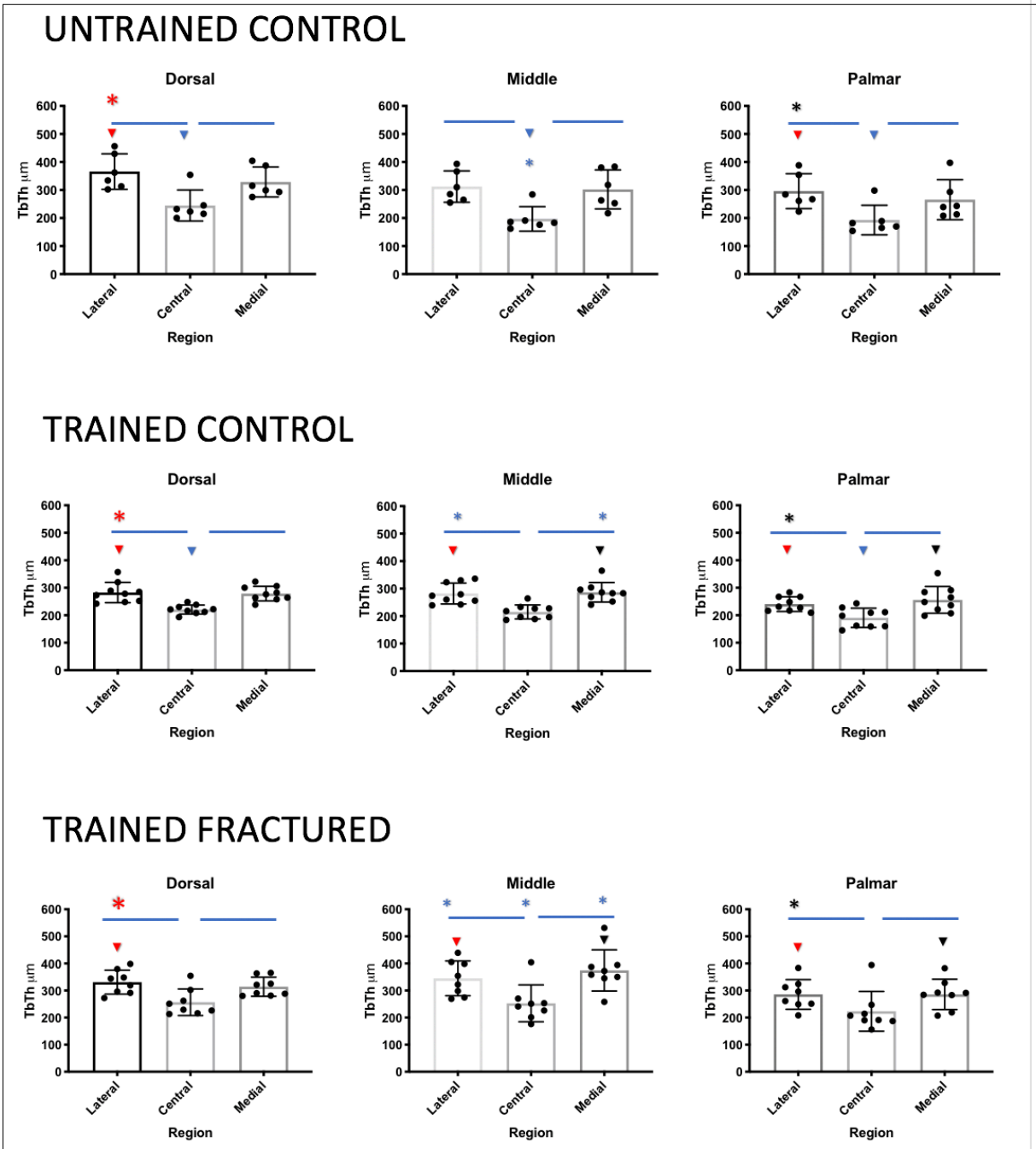

Figure 19: Scatter plots with bar showing the trabecular thickness (Tb.Th) results. The significant difference in Tb.Th from the lateral to medial aspects, within groups, is reported with a blue bar above the columns. The significant difference in Tb.Th from the dorsal to palmar aspect, within groups, is reported with a down-pointing triangle (▼). Red= lateral; Blue = central; Black = medial. The significant difference in Tb.Th between the 3 groups is indicated by an asterisk (*). Red= dorsal; Blue= middle; Black = palmar.

WITHIN GROUPS

When assessed on a frontal plane, in all three groups, the Tb.Th is significantly higher in the lateral (UC dorsal p=0.004, UC middle p=0.01, UC palmar 0.002, TC dorsal p=0.0007, TC middle p=0.002, TC palmar 0.006, TF dorsal p=0.001, TF middle p=0.01, TF palmar 0.001) and medial (UC dorsal p=0.01, UC middle p=0.006, UC palmar 0.003, TC dorsal p=0.0008, TC middle p=0.006, TC palmar 0.002, TF dorsal p=0.003, TF middle p=0.03, TF palmar 0.005) aspects compared to central aspect.

When assessed on a sagittal plane, the Tb.Th of the UC group is significantly higher in the dorsolateral compared to the palmarolateral aspect (p=0.01) and in the dorsocentral aspect compared to the middlecentral (p=0.006) and palmarocentral aspects (p<0.0001). A similar pattern was noted in the TC group, where the Tb.Th was significantly higher in the dorsolateral (p=0.006) and middlelateral (p=0.002) aspect compared to the palmarolateral aspect , in the dorsocentral aspect compared to the palmarocentral aspect (p=0.02) and in the middlemedial compared to the palmaromedial aspect (p=0.02). Similarly, in the TF group, the Tb.Th is significantly higher in the dorsolateral (p=0.008) and middlelateral (p=0.008) aspect compared to the palmarolateral aspect and in the middlemedial compared to the palmaromedial aspect (p=0.01).

BETWEEN GROUPS

In the dorsolateral region of the sagittal groove, the Tb.Th is significantly higher in the UC compared to the TC group (p=0.01). In the same region, the Tb.Th tends to be higher in the TF compared to the TC group (p=0.1).

In the middlemedial region, the Tb.Th is significantly higher in the TF compared to the TC (p=0.04). In the middlelateral region, the Tb.Th tends to be higher in the TF compared to the TC group (p=0.1). In the middlecentral region, the Tb.Th tends to be higher in the TF compared

to the UC group (p=0.1). In the palmarolateral region, the Tb.Th tends to be higher in the UC (p=0.09) and in the CF group (p=0.1) compared to the TC group.

TBB VOI	UC		TC		TF	
	Mean	SD	Mean	SD	Mean	SD
VOI 10	3.66E+02	63.3172011	2.83E+02	36.7500994	3.31E+02	44.3516291
VOI 11	2.45E+02	55.636948	2.21E+02	16.3991219	2.56E+02	49.0506481
VOI 12	3.29E+02	53.4568299	2.79E+02	26.7061688	3.14E+02	35.1043045
VOI 13	3.12E+02	55.9643664	2.82E+02	38.0715734	3.45E+02	64.2340788
VOI 14	1.97E+02	44.0102458	2.15E+02	25.5961798	2.53E+02	68.0846194
VOI 15	3.03E+02	69.2940313	2.87E+02	35.4829665	3.74E+02	75.9255884
VOI 16	2.96E+02	62.3526803	2.41E+02	26.5187995	2.86E+02	54.6442332
VOI 17	1.93E+02	52.9866742	1.90E+02	34.8923667	2.23E+02	73.6952728
VOI 18	2.65E+02	71.0756028	2.56E+02	48.7800222	2.86E+02	55.8165851

Table 6 – Means and standard deviations for Trabecular Bone Thickness (Tb.Th, units of µmg)

4.3.4 Trabecular Separation

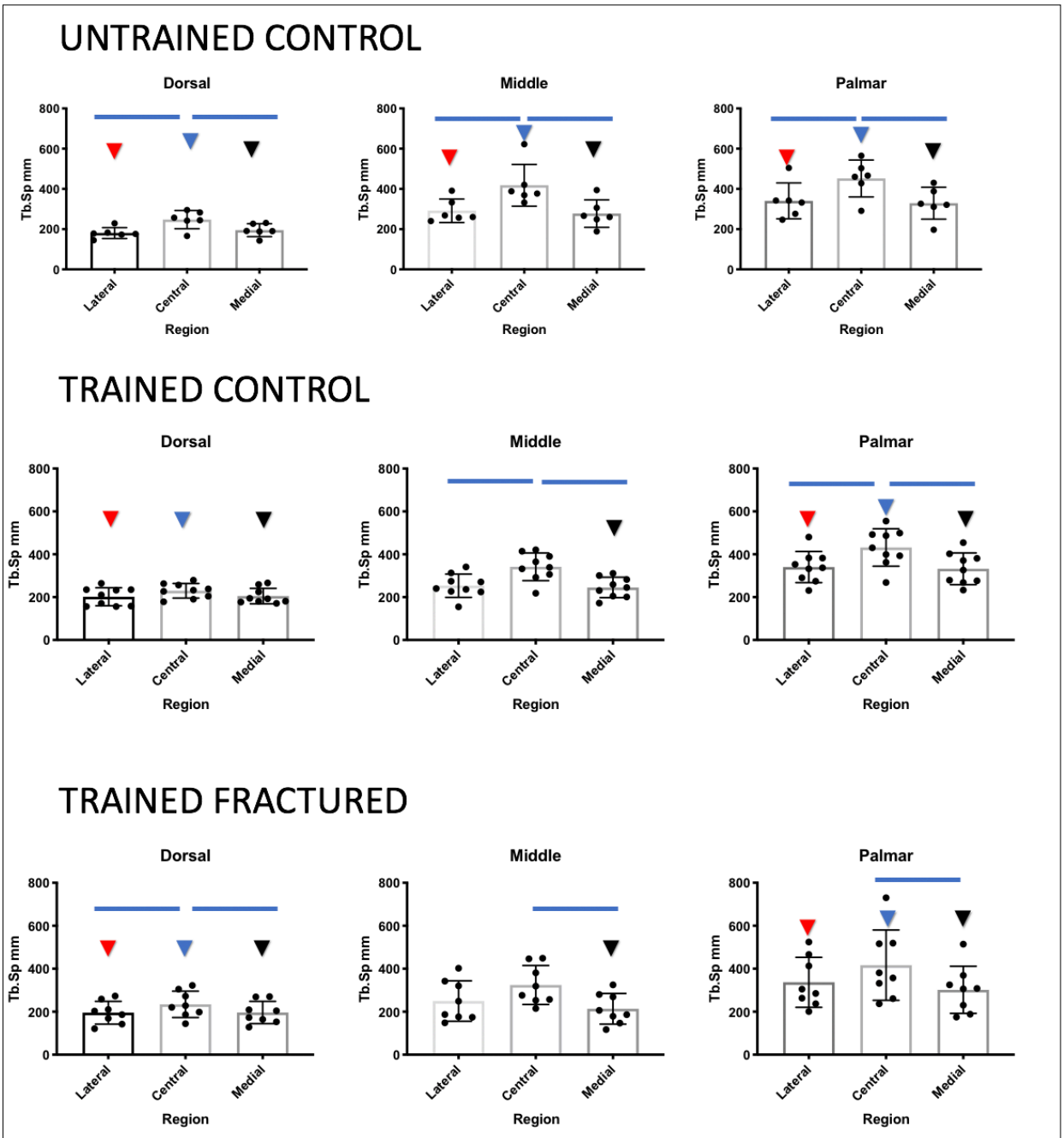

Figure 20: Scatter plots with bar showing the trabecular separation (Tb.Sp) results. The significant difference in Tb.Sp from the lateral to medial aspects, within groups, is reported with a blue bar above the columns. The significant difference in Tb.Sp from the dorsal to palmar aspect, within groups, is reported with a down-pointing triangle (▼). Red= lateral; Blue = central; Black = medial. The significant difference in Tb.Sp between the 3 groups is indicated by an asterisk (*). Red= dorsal; Blue= middle; Black = palmar.

WITHIN GROUPS

When assessed in a frontal plane, in the UC group, the Tb.Sp is significantly lower in the lateral and medial aspects compared to the central aspect. This is noted in the dorsal, middle and palmar aspects (dorsolateral p=0.006, middlelateral p=0.03, palmarolateral p=0.005, dorsomedial p=0.02, middlemedial p=0.001, palmaromedial p=0001). A similar pattern is noted in the TC and TF group, except for the dorsal aspect of the sagittal groove, where , no significant difference in Tb.Sp was noted. In the TC group, in the middle and palmar regions, the Tb.Sp is significantly lower in the lateral (middle p=0.002, palmar p=0.01) and medial (middle p=0.006, palmar=0.01) aspect compared to the central aspect. In the TF group, in the middle and palmar regions, the Tb.Sp is significantly lower in the lateral (middle p=0.07, palmar p=0.008) and medial (middle p=0.07, palmar=0.008) aspect compared to the central aspect.

When assessed from the dorsal to palmar aspect, the Tb.Sp tends to be lower dorsally and higher palmarly in all three groups. In the UC group, in the lateral, central and medial aspect of the sagittal groove, the Tb.Sp. is significantly lower dorsally compared to the middle (lateral p=0.002, central p=0.007, medial p=0.04) and palmar (lateral p=0.004, central p=0.0004, medial p=0.005) region. In both TC and TF groups, in the lateral, central and medial aspect of the sagittal groove, the Tb.Sp is significantly lower dorsally compared to the palmar aspect (TC lateral p=0.0002, TC central p<0.0001, TC medial p=0.0005, TF lateral p=0.0005, TF central p=0.0005, TC medial p=0.005).

BETWEEN GROUPS

In the middle medial region, the Tb.Sp tends to be lower in the TF group compared to the UC group, however, no significant difference is noted (p=0.1).

TBB VOI	UC		TC		TF	
	Mean	SD	Mean	SD	Mean	SD
VOI 10	1.81E+02	27.3097233	2.02E+02	41.7234284	1.95E+02	52.8124028
VOI 11	2.48E+02	45.4590195	2.30E+02	33.8043374	2.34E+02	60.9770933
VOI 12	1.95E+02	31.8090738	2.05E+02	36.1123081	1.96E+02	52.0229276
VOI 13	2.92E+02	58.4478334	2.53E+02	54.3091713	2.50E+02	94.260268
VOI 14	4.18E+02	103.855671	3.42E+02	65.0173514	3.24E+02	90.5397254
VOI 15	2.77E+02	68.2789121	2.45E+02	47.6346934	2.14E+02	71.3455434
VOI 16	3.40E+02	89.3226187	3.40E+02	72.7356649	3.37E+02	116.496379
VOI 17	4.52E+02	91.6470232	4.32E+02	87.06172	4.17E+02	163.616056
VOI 18	3.29E+02	79.1825461	3.32E+02	73.8500023	3.02E+02	109.811101

Table 7 – Means and standard deviations for Trabecular Trabecular Separation (Tb.Sp, units of μmg)

4.3.5 Trabecular Number

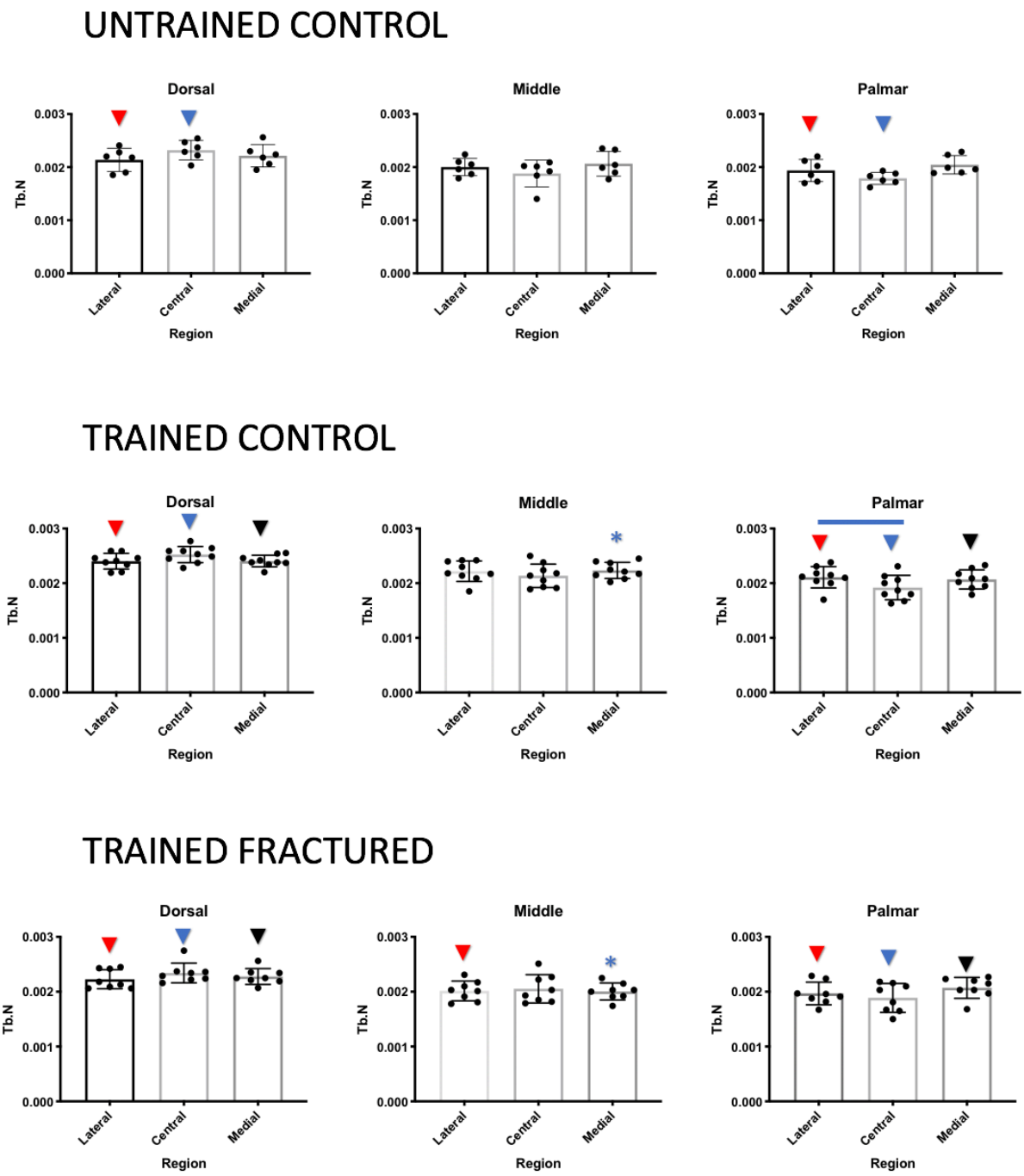

Figure 21: Scatter plots with bar showing the trabecular number (Tb.N) results. The significant difference in Tb.N from the lateral to medial aspects, within groups, is reported with a blue bar above the columns. The significant difference in Tb.N from the dorsal to palmar aspect, within groups, is reported with a down-pointing triangle (▼). Red= lateral; Blue = central; Black = medial. The significant difference in Tb.N between the 3 groups is indicated by an asterisk (*). Red= dorsal; Blue= middle; Black = palmar.

WITHIN GROUPS

When assessed in a frontal plane, no significant differences in Tb.N are detected across the sagittal groove in the UC and TF groups. However, in the TC group, the Tb.N was significantly higher in the palmarolateral compared to the palmarocentral region (p=0.02).

When assessed in a sagittal plane, in the UC group, the Tb.N is significantly higher in the dorsolateral (p=0.02) and dorsocentral (p=0.01) region of the sagittal groove compared to the palmarolateral and palmarocentral region, respectively. This pattern is also noted in both TC and TF group (TC dorsolateral p=0.002, TC dorsocentral p=0.0002, TF dorsolateral p=0.001, TF dorsocentral P=0.0003). However, in these 2 groups, the Tb.N is also significantly higher in the dorsomedial compared to the palmaromedial region (TC p=0.0002, TF p=0.05).

BETWEEN GROUPS

In the middlemedial region, the Tb.N is significantly higher in the TC compared to the TF group (P=0.04). The Tb.N tends to be higher in the TC group compared to the TF and UC groups in the dorsal regions of the sagittal groove (TF lateral p=0.1, TF central p=0.06, UC lateral p=0.05, UC central 0.1, UC medial p=0.06).

TBB VOI	UC		TC		TF	
	Mean	SD	Mean	SD	Mean	SD
VOI 10	2.14E-03	0.00021744	2.40E-03	0.00014275	2.23E-03	0.00017411
VOI 11	2.32E-03	0.00018364	2.52E-03	0.00014621	2.34E-03	0.00017894
VOI 12	2.22E-03	0.00020999	2.40E-03	0.00010736	2.28E-03	0.00014546
VOI 13	2.00E-03	0.00016313	2.22E-03	0.00018712	2.01E-03	0.0001789
VOI 14	1.88E-03	0.00024841	2.14E-03	0.0002152	2.05E-03	0.00025616
VOI 15	2.06E-03	0.00023297	2.23E-03	0.00014598	2.00E-03	0.00015601
VOI 16	1.94E-03	0.00020716	2.11E-03	0.00019508	1.97E-03	0.000207
VOI 17	1.79E-03	0.00011275	1.92E-03	0.00022368	1.89E-03	0.00026346
VOI 18	2.04E-03	0.00017299	2.07E-03	0.00017494	2.07E-03	0.00019115

Table 8 – Means and standard deviations for Trabecular Number (Tb.N, units of 1/µmg)

4.3.6 Connectivity Density

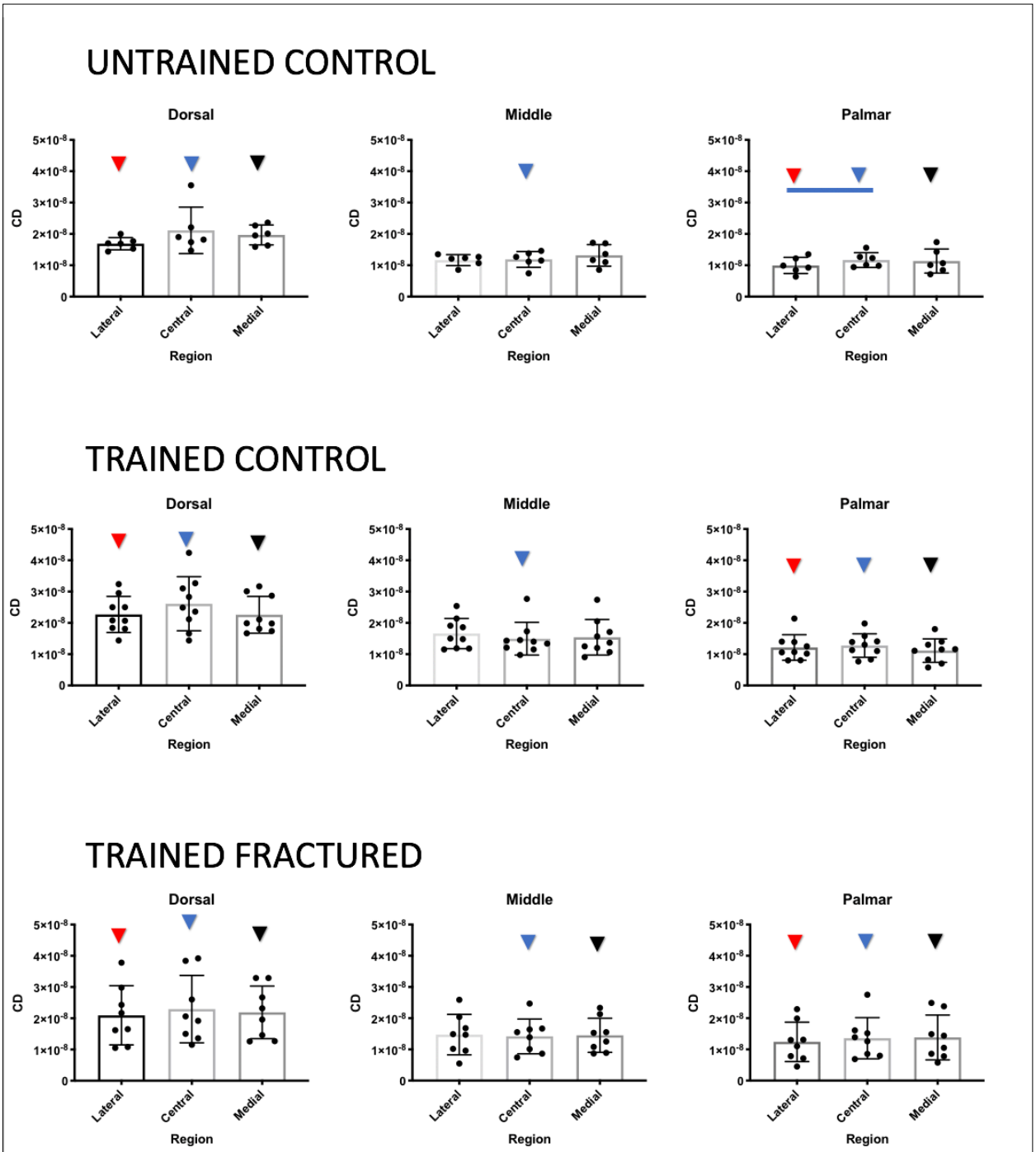

Figure 22: Scatter plots with bar showing the Connectivity Density (Conn.D) results. The significant difference in Conn.D from the lateral to medial aspects, within groups, is reported with a blue bar above the columns. The significant difference in Conn.D from the dorsal to palmar aspect, within groups, is reported with a down-pointing triangle (▼). Red= lateral; Blue = central; Black = medial. The significant difference in Conn.D between the 3 groups is indicated by an asterisk (*). Red= dorsal; Blue= middle; Black = palmar.

WITHIN GROUPS

When assessed in a frontal plane, in the UC group, the Connectivity Density (Conn.D) is significantly higher in the palmaro-central compared to the palmaro-lateral region ($p<0.05$). In the TC and TF groups, no significant differences in Conn.D were noted on a frontal plane.

When assessed in a sagittal plane, in all three groups, the Conn.D in the lateral, central and medial aspect of the sagittal groove, is significantly higher in the dorsal regions compared to the palmar regions (UC lateral $p=0.004$, UC central $p=0.02$, UC medial $p=0.004$, TC lateral $p<0.0001$, TC central $p=0.002$, TC medial $p<0.0001$, TF lateral $p=0.0005$, TF central $p=0.001$, TF medial $p=0.001$). The Conn.D is also significantly higher in the dorsocentral compared to the middle central region (UC $p=0.02$, TC $p=0.01$, TF $p=0.03$). Only in the TF group, the Conn.D in the dorsomedial region is significantly higher compared to both the middlemedial ($p=0.03$) and palmaromedial ($p=0.001$) regions.

BETWEEN GROUPS

No statistically significant differences in Conn.D are noted between groups. However, in the dorsolateral region of the sagittal groove, the Conn.D tends to be higher in the TC group compared to the UC group ($p=0.1$).

TBB VOI	UC		TC		TF	
	Mean	SD	Mean	SD	Mean	SD
VOI 10	1.69E-08	1.9641E-09	2.27E-08	5.7786E-09	2.10E-08	9.4673E-09
VOI 11	2.12E-08	7.4037E-09	2.61E-08	8.6459E-09	2.29E-08	1.076E-08
VOI 12	1.97E-08	3.1768E-09	2.26E-08	5.895E-09	2.19E-08	8.4198E-09
VOI 13	1.17E-08	1.7728E-09	1.66E-08	4.84E-09	1.48E-08	6.4915E-09
VOI 14	1.19E-08	2.5211E-09	1.50E-08	5.2147E-09	1.42E-08	5.5653E-09
VOI 15	1.32E-08	3.4497E-09	1.54E-08	5.6933E-09	1.45E-08	5.457E-09
VOI 16	9.96E-09	2.5744E-09	1.22E-08	4.0813E-09	1.24E-08	6.3155E-09
VOI 17	1.17E-08	2.3407E-09	1.28E-08	3.7495E-09	1.36E-08	6.593E-09
VOI 18	1.13E-08	3.8271E-09	1.12E-08	3.7654E-09	1.38E-08	7.1839E-09

Table 9– Means and standard deviations for trabecular bone Connectivity Density (Conn.D, units of $1/\mu m^3$)

4.3.7 Degree of Anisotropy

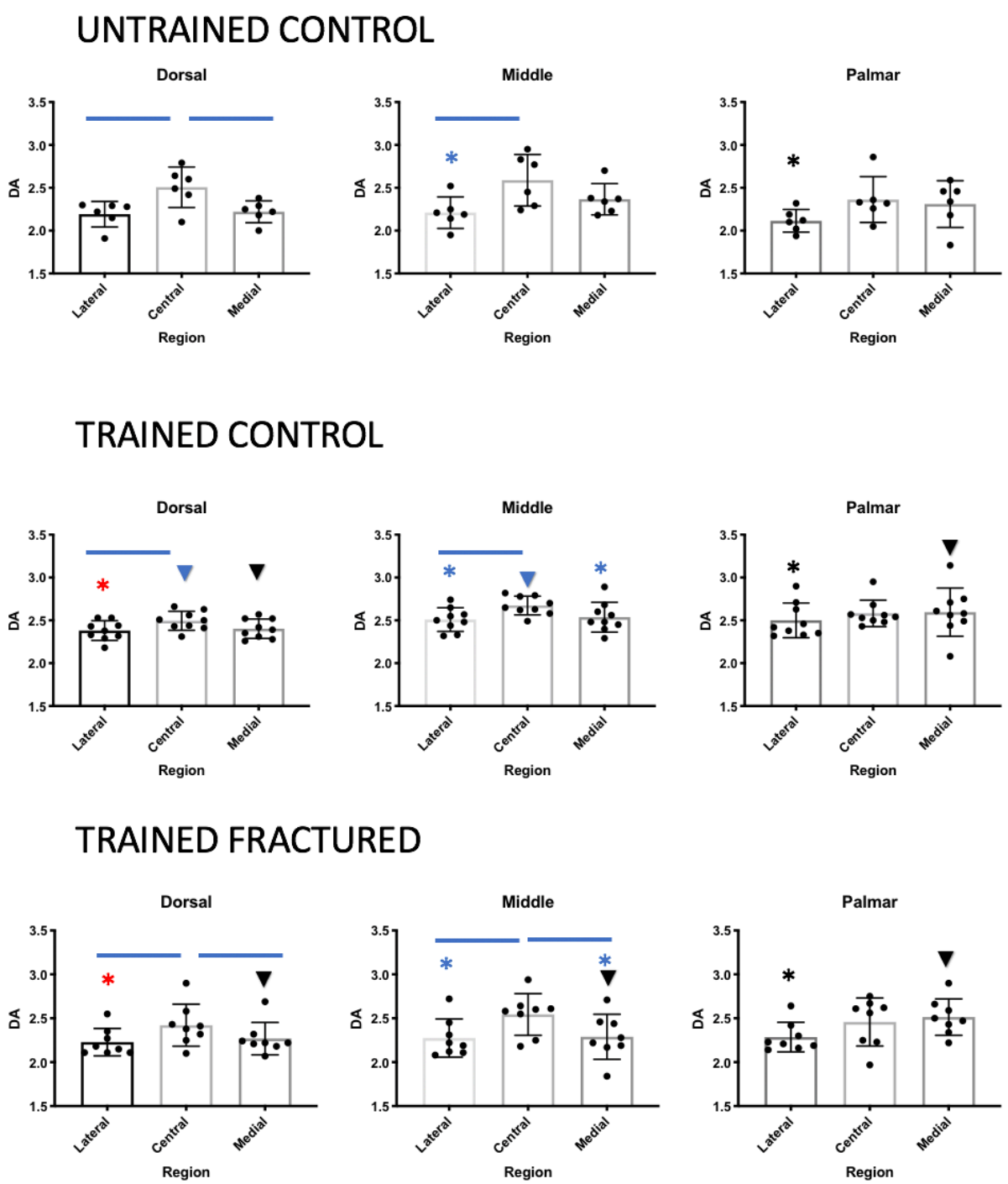

Figure 23: Scatter plots with bar showing the Degree of Anisotropy (DA) results. The significant difference in DA from the lateral to medial aspects, within groups, is reported with a blue bar above the columns. The significant difference in DA from the dorsal to palmar aspect, within groups, is reported with a down-pointing triangle (▼). Red= lateral; Blue = central; Black = medial. The significant difference in DA between the 3 groups is indicated by an asterisk (*). Red= dorsal; Blue= middle; Black = palmar.

WITHIN GROUPS

For the dorsal and middle region of each group, the DA was higher centrally compared to lateral (UC dorsal p=0.02, UC middle p=0.004, TC dorsal p=0.02, TC middle p=0.006, TF dorsal p=0.02, TF middle p=0.03). In the UC and TF groups, the DA was higher centrally compared to medial for the middle region also (UC p=0.02, TF p=0.02). No significant differences in DA are noted between the medial, central and lateral sites palmarly.

When assessed on a sagittal plane, in the UC group, there are no significant differences in DA. However, there were some differences noted in the race-trained groups. In the TC group, the DA in the central aspect of the sagittal groove is significantly higher in the middle compared to the dorsal region (p=0.02). In the medial aspect of the sagittal groove, the DA is significantly higher in the palmar compared to the dorsal aspect (p=0.02). In the TF group, in the medial aspect of the sagittal groove , the DA in the palmar aspect is significantly higher compared to both the dorsal (p=0.03) and middle (p=0.01) aspect.

BETWEEN GROUPS

The DA is significantly higher in the TC group compared to the TF group in the dorso-lateral (p=0.05) and middle-medial (p=0.05) aspect of the sagittal groove. Moreover, the DA is significantly higher in the TC group compared to both the UC and the TF groups in the middle-lateral (TC-UC p=0.03, TC-TF p=0.03) and palmaro-lateral aspect (TC-UC p=0.001, TC-TF p=0.05) of the sagittal groove.

TBB VOI	UC		TC		TF	
	Mean	SD	Mean	SD	Mean	SD
VOI 10	2.19E+00	0.14675289	2.38E+00	0.11381587	2.22E+00	0.148354
VOI 11	2.51E+00	0.23453394	2.49E+00	0.11223023	2.41E+00	0.22510332
VOI 12	2.22E+00	0.12876287	2.40E+00	0.11514542	2.26E+00	0.17728628
VOI 13	2.21E+00	0.18355846	2.51E+00	0.13680146	2.23E+00	0.24914685
VOI 14	2.59E+00	0.3005244	2.67E+00	0.10855191	2.52E+00	0.23199442
VOI 15	2.37E+00	0.18342776	2.54E+00	0.17429543	2.28E+00	0.24071933
VOI 16	2.12E+00	0.13265905	2.50E+00	0.20239481	2.24E+00	0.20841491
VOI 17	2.36E+00	0.26705621	2.58E+00	0.15310395	2.44E+00	0.26126991
VOI 18	2.31E+00	0.27180423	2.60E+00	0.28120149	2.48E+00	0.21751399

Table 10– Means and standard deviations for trabecular bone Degree of Anisotropy (DA)

Chapter 5

Discussion

1632 This study analyses the microstructural characteristics (density and architecture) of the
1633 subchondral (SCB) and trabecular (TB) bone of the proximal sagittal groove (PSG) of the PP in
1634 horses with different training history (racing and non-racing) and injury status (with and
1635 without a proximal phalangeal fracture).
1636 We found that the microstructural characteristics of the subchondral and trabecular bone vary
1637 across the dorsopalmar and lateromedial aspect of the PSG; however, contrary to our
1638 hypothesis, these variations are noted in all three groups and not only in the TF group. On the
1639 other hand, significant differences in SCB and TB microstructural characteristics were noted
1640 between the three groups.
1641 Significant differences in SCB and TBB TMD were noted transversally and longitudinally across
1642 the sagittal groove in all three groups. This finding provides only partial support for our
1643 hypothesis because significant differences in SCB TMD were detected in all three groups, not
1644 only in the race-trained fractured group (TF). However, within the UC group, a significant
1645 difference in SCB TMD was noted only within the palmar aspect, in contrast to the race-trained
1646 horses (TF and TC), where significant differences in SCB TMD were noted within the palmar
1647 and the dorsal aspects of the joint. The pattern of different SCB TMD dorsally is consistent
1648 with the higher loads experienced by the metacarpophalangeal joint in the race-trained
1649 groups compared to the UC group. During the stance phase, the contact area between the
1650 distal aspect of the third metacarpal bone and the proximal aspect of the proximal phalanx is
1651 located slightly towards the palmar/plantar edge of the joint surface, with a relatively large
1652 non-contact area at the dorsal articular margin. When the sagittal plane load is increased to
1653 10,500N, mimicking the gallop, the dorsolateral and dorsomedial joint margins come into full
1654 contact (Brama et al. 2001). Therefore, the dorsal aspect of the sagittal groove of race-trained
1655 horses is subjected to higher loading compared to horses that never experience race training.

1656 The differences in TMD across the sagittal groove may be explained by presence of focal areas
1657 of remodeling, where bone resorption is occurring, in the regions of increased contact
1658 between the distal MC3 and PP. Considering that significant differences in TMD are noted in
1659 all three groups, presence of a gradient of density within the sagittal groove is unlikely to be
1660 a predisposing factor for proximal phalangeal fractures.
1661 Both within the subchondral bone and the trabecular bone layers, the tissue mineral density
1662 is significantly higher in the TF group compared to the TC group. Similarly, BV/TV is significantly
1663 higher in the middle-central region of TF group compared to the TC and UC groups. These
1664 findings partially support our hypothesis that microstructural characteristics of the PSG vary
1665 significantly between TF and TC group. No significant difference in TMD was noted between
1666 the trained control and the untrained group or between the trained control and the untrained
1667 group. This finding is in contrast with our hypothesis that an increased bone density is noted
1668 in both race-trained groups compared to the untrained group. The increase in bone density in
1669 the TF group may be explained by an increased modelling coupled to reduced remodelling
1670 occurring in SCB and TB of horses that experienced proximal phalangeal fracture. Regular
1671 strenuous exercise has been reported to inhibit remodelling in young Thoroughbreds and
1672 human endurance athletes (Firth et al. 2005, McCarthy et al. 1992) leading to a higher degree
1673 of tissue mineralization. Excessive/increased mineralization increases bone stiffness and
1674 strength; while also, leading to reduced toughness and increased susceptibility to fractures,
1675 especially in high energy events. Our data showing that BV/TV is greater in specific VOI of TF
1676 bones is similar to previous post mortem studies on proximal sesamoid bones reporting an
1677 increased BV/TV of fractured proximal sesamoid bones as compared to both control
1678 racehorses and horses living at pasture (Cresswell et al. 2019, Peloso et al. 2015, Anthenill et
1679 al. 2010, Young et al. 1991). In Cresswell's study (2019), the palmar surface of the sesamoid

1680 bones, where fracture most likely initiates, had the greatest increase in BV/TV, highlighting
1681 the association between increased BV/TV and fracture pathology. Similar findings were
1682 reported by multiple studies investigating the distal metacarpal condyles of racing
1683 Thoroughbreds, where fatigue damage is mainly located in areas of increased bone volume
1684 fraction (Norrdin and Stover 2006, Rubio-Martinez et al. 2008, Muir et al. 2006; Whitton et al.
1685 2018). Whitton et al. (2010) reported that horses that had fracture of the third metacarpal
1686 condyle had less porous condylar SCB and higher BV/TV at the fracture sites. Contrary to
1687 Whitton's study, our results did not show statistically significant differences in TP between the
1688 three groups. However, racehorses that sustained a proximal phalangeal fracture *tended* to
1689 have increased SCB TP in the dorsomedial and dorsolateral aspects of the sagittal groove
1690 compared to the UC**.** This finding is in contrast with the fact that an overall increased bone
1691 density is noted in the TF group. Assuming that focal porosity is related to areas of bone
1692 resorption due to remodelling secondary to a period of rest or to microcracks accumulation,
1693 then increased porosity may weaken the bone at a focal point, increasing the risk of fracture.
1694 In human medicine, cortical porosity has recently been proposed as a quantifiable marker of
1695 bone loss and bone fragility that can be used by the clinician to identify bones at risk for
1696 fracture (Bala et al. 2015). Significant differences in subchondral bone total porosity were
1697 noted transversally and longitudinally across the sagittal groove within all three groups. This
1698 finding is in contrast with our hypothesis that significant differences would be noted in the TF
1699 group but not in the UC and TC groups. Total porosity was consistently lower in the middle
1700 compared to the dorsal and palmar aspects of the sagittal groove in all three groups. Similarly
1701 the TMD was higher in the middle compared to the dorsal and palmar aspects of the sagittal
1702 groove in all three groups.

When assessed in a frontal plane, the BV/TV was consistently lower in the central regions compared to the lateral and medial regions in all three groups. When assessed on a sagittal plane, the BV/TV decreases from dorsal to palmar in all three groups. These findings are in contrast with our hypothesis stating that microstructural characteristics of the PSG varies significantly across its dorsopalmar and lateromedial aspect in the TF group but not in the UC and TC groups.

The architecture of cancellous bone can be characterized by number, thickness, separation and connectivity density (Burr 2014). Each of these factors contributes to the overall cancellous bone volume, but the same bone volume can contain trabeculae that are organized in different ways (i.e. more trabeculae that are thinner or fewer, thicker trabeculae). Our data shows that, in all three groups, the Tb.Th., Tb.N. and Connectivity Density decrease from the dorsal to palmar aspect of the PSG. On the other hand, the trabecular separation increases from the dorsal to palmar aspect. Again, these findings are in contrast with our hypothesis stating that the bone microstructural characteristics vary significantly across the dorsopalmar and lateromedial aspect of the PSG of TF group but not TC and UC groups. However, when the architecture parameters were compared between the different groups, it was noted that the TbTh, similarly to the BV/TV, is significantly higher in the middlecentral region of TF group compared to the other groups**.** Moreover, the TF group *tends* to have lower trabecular separation, trabecular number and connectivity density compared to the TC group. These findings support our hypothesis, since evidence of trabecular bone disruption is noted in the TF but not on the TC group. Horses that experienced a proximal phalangeal fracture have higher bone density, higher BV/TV and higher Tb.Th, but lower trabecular separation, trabecular number and connectivity density compared to horses that did not experience a fracture. It has been shown that the loss of complete trabeculae (reducing Tb.N) reduces the

strength and stiffness of bone by two to three times more than does losing the same amount of bone via trabecular thinning (Burr 2014). The reason for the reduction in strength and stiffness is that the loss of whole trabeculae reduces connectivity within the entire structure, which makes the structure much less capable of bearing weight and less able to direct stresses to the cortex than does maintaining the connections but making them thinner (Burr 2014).

The degree of anisotropy (DA) of the trabecular bone is a measure of how highly oriented trabeculae are within the bone volume. Trabecular bone adapts its orientation depending on mechanical load and can become anisotropic. Instead of being homogeneously distributed and randomly oriented (isotropy) within a whole bone specimen, trabeculae are strategically positioned, conferring upon the bone its anisotropic characteristics. Trabeculae are oriented along the principal directions of forces within the bone, making the bone stronger in that particular loading direction (Lanyon 1987). Our study shows that there are significant variations in DA of the PSG on a sagittal plane of race-trained horses but not of untrained horses. In race-trained horses, the DA is significantly higher in the dorsal regions. Since the DA provides insight into the directional dependence of bone strength and the dorsal aspect of the sagittal groove of race-trained horses is subjected to higher loading compared untrained horses, it is not surprising that the DA is significantly higher dorsally compared to the middle and palmar regions in race-trained horses (Turner 1992). This finding partially supports our hypothesis that microstructural differences are noted across the PSG in the TF, but not in UC.

In the TC group, the DA was overall significantly higher, compared to both the TF and the UC groups. An increased DA in the TC group may indicate a better organization and a positive adaptation of the trabecular bone to race-training. The more isotropic microstructure of the trabecular bone in the TF group can be explained by a higher degree of sclerosis as evidenced by an increase in bone volume fraction caused by the narrowing and filling in of marrow spaces

(Boyde 1999). A lower DA, together with a lower trabecular number and connectivity density may indicate an overall sclerotic but poorly organized trabecular bone that is less capable of load bearing, less able to direct stresses to the cortex and has not positively adapted to race-training.

Overall, the results demonstrate the presence of some prodromal microstructural changes within the PSG of TF group. An increased subchondral bone density along with trabecular thickening and disruption of the trabecular bone architecture, may predispose the horse to PP fracture and may represent an inadequate adaptation to race-training. Our data support previously reported clinical findings suggesting that sagittal proximal phalangeal fractures are of the fatigue type. Smith et al (2014) reported an increased thickness of the subchondral bone of the proximal aspect of the PP in Thoroughbred racehorses that experience sagittal PP fracture. Powell (2012) described trabecular bone mineral densification around the fracture line in 4 of 19 Thoroughbred racehorses diagnosed by MRI to have short incomplete parasagittal fractures of the proximal phalanx.

The current scientific evidence, including the data obtained in this study, suggest that sagittal proximal phalangeal fractures occur in horses that respond to race-training by continued bone modelling in the face of suppressed remodeling. Inhibition of remodelling may allow accumulation of fatigue damage that can ultimately result in fracture. Further histological studies are necessary to confirm the above statement. In particular presence of osteoid, reversal lines (both indicators of remodelling) and microcracks within the PSG of horses with different training history and injury status should be explored using histomorphometry.

This study has multiple limitations. Firstly, the sample size is modest. The training and medical history of each horse included in the study is unknown. Previous studies showed that training is one of the most important modifiable variables affecting the risk of musculoskeletal injury

in racehorses (Boston et al 2000, Boden et al. 2007a, Boden et al. 2007b). Knowing the different training regimes of the horses included in the study, would have helped understanding why some horses developed a functional adaptation to race-training and why some did not. Based on our findings, it is not possible to determine why some race-trained horses have an increased tissue mineral density, increased BV/TF poor trabecular architecture and decreased DA compared to others. It can be a subjective "poor" adaptation to race training or it can be the results of training methods that do not allow functional adaptation to the abnormal loads. Although the racehorses included in the study were racing at the time of their injury, the pre-race soundness was not and could not be assessed, so any evidence of pre-facture lameness was not available.

Horses included in the TF group were euthanized due to presence of a comminuted proximal phalangeal fracture. According to Ramzan (2011), the most common configuration of proximal phalangeal fractures in the UK is the incomplete. Another limitation of our study is that our sample population may not be a truly representative population of horses with proximal phalangeal fractures. Horses with an incomplete proximal phalangeal fracture are more common and carry an overall good prognosis following repair and they are less likely to be euthanized compared to horses with a comminuted proximal phalangeal fracture.

The imaging modality used in this study is not applicable to clinical setting. The main risk parameters identified in our study cannot be readily determined in a living horse. This is the main barrier to application of the study findings to clinical practice.

In conclusion race-trained horses that have sustained a proximal phalangeal fracture have an increased SCB density, increased trabecular thickness, reduced trabecular number, trabecular separation, and trabecular connectivity within the proximal sagittal groove region. These

findings would support the theory that an inadequate adaptive bone response within the proximal sagittal groove might contribute to sagittal fractures of the first phalanx. Identification of the horse at increased risk of proximal phalangeal fracture remains a challenge, however, advanced imaging modalities available in clinical setting, such as gamma scintigraphy, magnetic resonance imaging and computed tomography are useful in identifying early signs of osseous damage within the proximal aspect of the proximal phalanx.

References

- Alexander, R.McN. (1984) Elastic energy stores in running vertebrates. American Zoologist. 24, pp. 85-94
- Allen, M.R. and Burr, D.B. (2008) Skeletal microdamage: less about biomechanics and more about remodeling. Clin Rev Bone Miner Metabol. 6, pp. 24–30.
- Allen, M.R. and Burr, D.B. (2014) Bone Modeling and Remodeling. In: “Basic and applied bone biology”. Eds: Burr, D.B and Allen, M.R., Elsevier.
- Anthenill, L.A., Gardner, I.A. and Pool, R.R. (2010) Comparison of macrostructural and microstructural bone features in thoroughbred racehorses with and without midbody fracture of the proximal sesamoid bone. Am. J. Vet. Res. 71, p.755.
- Augat, P. and Schorlemmer, S. (2006) The role of cortical bone and its micro- structure in bone strength. Age Ageing. 35 Suppl 2:ii pp.27–31.
- Bailey, E., Petersen, J.L. and Kalbfleischs, T.S. (2022) Genetics of Thoroughbred racehorse performance. Annual Review of Animal Biosciences. 10, p131.
- Bala, Y., Zebaze, R., Seeman, E. (2015) Role of cortical bone in bone fragility. Curr Opin Rheumatol. 27(4) pp406–13.
- Barone, R. (1995) Anatomie Comparée des mammiféres domestiques. Tome 1, Osteologie. Ed. VIGOT.
- Bathe, A.P. (1994) 245 Fractures in Thoroughbred racehorses: results of a 2-year prospective study in Newmarket. Proc. Am. Assoc. Equine Practnrs. 40, pp.175.
- Bentolila, V., Boyce, T.M., Fyhrie, D.P., et al. (1998) Intracortical remodeling in adult rat long bones after fatigue loading. Bone 23(3), pp. 275–281.

1845 – Biewener, A.A., Thomason, J., Goodship, A. et al. (1983) Bone stress in the horse
1846 forelimb during locomotion at different gaits: A comparison of two experimental methods.
1847 Journal of biomechanics. 16(8), pp. 565–576.
1848 – Boden, L.A., Anderson,G.A. et al. (2007a) Risk factors for Thoroughbred racehorse
1849 fatality in flat starts in Victoria (1989-2004). Equine Vet. J. 39(5), pp 430-437.
1850 – Boden, L.A., Anderson,G.A. et al. (2007b) Risk factors for Thoroughbred racehorse
1851 fatality in jump starts in Victoria (1989-2004). Equine Vet. J. 39(5), pp 422-428.
1852 – Boston, R.C. and Nunamaker, D.M. (2000) Gait and speed as exercise components of
1853 risk factors associated with onset of fatigue injury of the third metacarpal bone in 2-year-old
1854 Thoroughbred racehorses. Am. J. Vet. Res. 61(6), pp.602–608.
1855 – Bouxsein M.L., Boyd S.K., Christiansen B.A., Guldberg R.E., Jepsen K.J., Müller R. (2010)
1856 Guidelines for assessment of bone microstructure in rodents using micro-computed
1857 tomography. J Bone Miner Res. 25(7), pp.1468-86.
1858 – Boyde A, Haroon Y, Jones SJ, et al. (1999) Three dimensional structure of the distal
1859 condyles of the third metacarpal bone of the horse. Equine Vet J. 31, pp.122–129.
1860 – Brama, P., Karssenberg, D., Barneveld, A., van Weeren, P.R. (2001) Contact areas and
1861 pressure distribution on the proximal articular surface of the proximal phalanx under sagittal
1862 plane loading. Equine Vet. J. 33 (1), pp. 26-32.
1863 – Buenzli, P.R., Sims, N.A., 2015. Quantifying the osteocyte network in the human
1864 skeleton. Bone 75, pp. 144-150.
1865 – Burr, D.P. and Akkus, O. (2014) Bone Morphology and Organization. In: “Basic and
1866 applied bone biology”. Eds: Burr, D.B and Allen, M.R., Elsevier.

– Bukowiecki, C.F., Bramlage, L.R., Gabel, A.A. (1987) In vitro strength of the suspensory apparatus in training and in resting horses. Veterinary Surgery, 16. pp.126-130.

– Cao, W., Helder, M.N., Brevenboer, N., Wu, G., Jin,J. et al. (2020) Is there a governing role of osteocytes in bone tissue regeneration? Curr. Osteoporos. Rep. 18(5), pp. 541-550.

– Casez, J.P., Fischer, S., Stussi, E., Stalder, H., et al. (1995) Bone mass at lumbar spine and tibia in young males – impact of physical fitness, exercise, and anthropometric parameters: a prospective study in a cohort of military recruits. Bone. 17, pp. 211-219.

– Clayton, H.M., Sha, D., Stick, J., Elvin, N. (2007) 3D kinematics of the equine metacarpophal- angeal joint at walk and trot. Vet. Comp. Orthop. Traumatol. 2, pp. 86-91.

– Cooper, D.M.L., Kawalilak, C.E., Harrison, K., Johnston, B.D., and Johnston, J.D. (2016) Cortical Bone Porosity: What Is It, Why Is It Important, and How Can We Detect It? Curr. Osteoporos. Rep. 14 pp. 187-198

– Cresswell, E.N., McDonough, S.P., Palmer, S.E., Hernandex, C.J. and Reesink H.L. (2019) Can quantitative computed tomography detect bone morphological changes associated with catastrophic proximal sesamoid bone fracture in Thoroughbred racehorses? Equine Veterinary Journal 51 pp. 123–130

– Cullen, D.M., Smith, R.T., and Akhter, M.P. (2000) Time course for bone formation with long-term external mechanical loading. J Appl Physiol 88, pp. 1943-1948;

– Cullen, D.M., Smith, R.T., and Akhter, M.P. (2001) Bone-loading response varies with strain magnitude and cycle number. J Appl Physiol 91, pp. 1971-1976.

– Currey J.D. (1988) The effect of porosity and mineral content on the Young's modulus of elasticity of compact bone. J Biomech. 21(2) pp.131–9.

– Currey, J.D. 2001 (2001) Ontogenetic changes in compact bone material properties. In: Bone Biomechanics Handbook. Ed. Cowin, S.C. London CRC Press.

– Currey, J.D. and Shahar, R. (2013) Cavities in the compact bone in tetrapods and fish and their effect on mechanical properties. J Struct Biol, 183(2) pp.107–2

– Den Hartog, S.M., Back, W., Brommer, H., Van Weeren, P.R. (2009) In vitro evaluation of the metacarpophalangeal joint loading during simulated walk. Equine Vet. J. 41(3), pp. 214-217.

– Dyson S, Nagy A, Murray A. (2011) Clinical and diagnostic imaging findings in horses with subchondral bone trauma of the sagittal groove of the proximal phalanx. Vet Radiol Ultrasound. 52(6):596-604.

– Einhorn T. (1992) Bone strength: the bottom line. Calcif Tissue Int. 51, pp.333–339.

– Ellis, D.R., Simpson, D.J., Greenwood, R.E. and Crowhurst, J.S. (1987) Observations and management of fractures of the proximal phalanx in young Thoroughbreds. Equine Vet. J. 19, pp. 43-49.

– Fackelman, G. (1973) Sagittal fracture of the first phalanx (P1) in the horse: fixation by the lag screw principle. Vet. Med. Small Anim. Clin. 68, pp. 622-636.

– Firth, E.C., Delahunt, J., Wichtel, J.W., et al. (1999a) Galloping exercise induces regional changes in bone density within the third and radial carpal bones of Thoroughbred horses. Equine veterinary journal 31(2), pp. 111–115.

– Firth, E.C., Goodship, A.E., Delahunt, J., et al. (1999b) Osteoinductive response in the dorsal aspect of the carpus of young thoroughbreds in training occurs within months. Equine veterinary journal. Supplement 30, pp. 552–54.

– Firth, E.C., Rogers, C.W., Doube, M., Jopson, N.B. (2005) Musculoskeletal responses of 2-year-old Thoroughbred horses to early training. N Z Vet J. 53 pp.101-12.

– Fleck, C. and Eifler, D. (2003) Deformation behaviour and damage accumulation of cortical bone specimens from the equine tibia under cyclic loading. Journal of biomechanics. 36(2) pp. 179–189.

– Gold SJ, Werpy NM, Gutierrez-Nibeyro SD. (2017) Injuries of the sagittal groove of the proximal phalanx in warmblood horses detected with low-field magnetic resonance imaging: 19 cases (2007-2016). Vet Radiol Ultrasound. 00 Pp.1-10.

– Harrison, S., Whitton, R.C., Kawcak, C.E., Stover, S.M., Pandy, M.G. (2010) Relationship between muscle forces, joint loading and utilization of elastic strain energy in equine locomotion. J. Exp. Biol. 213, pp. 3998-4009.

– Harrison, S., Whitton, C.R., Kawcak, C., Stover, S., Pandy, M. (2014) Evaluation of a subject-specific finite-element model of the equine metacarpophalangeal joint under physiological load. Journal of Biomechanics. 47, pp. 65–73.

– Hill, W.G. (1988) Why aren't horses faster? Nature, 332(6166), p. 678.

– Holcombe, S.J., Schneider, R.K., Bramlage, L.R. et al. (1995) Lag screw fixaton of noncomminuted sagittal fractures of the proximal phalanx in racehorses: 59 cases (1973-1991). J. Am. Vet. Med. Assoc. 206, p. 1195.

– Jackson, B.F., Lonnell, C., Verheyen, K.L., et al. (2005) Biochemical markers of bone metabolism and risk of dorsal metacarpal disease in 2-year-old Thoroughbreds. Equine Vet. J. 37(1), pp. 87-91.

– Jee, W.S.S. and Li, X.J. (1990) Adaptation of cancellous bone to overloading in the adult rat: a single photon-absorptiometry and histomorphometry study. Anat. Rec. 227, pp. 418-426.

– Jee, W.S.S., Li, X.J. and Schaffler, M.B. (1991) Adaptation of diaphyseal structure with aging and increased mechanical usage in the adult rat: a histomorphometrical and

biomechanical study. Anat. Rec. 230, pp. 332-338.

– Kraus, Beth M.Richardson, Dean W.Nunamaker, David M.Ross, M. W. (2004) Management of comminuted fractures of the proximal phalanx in 37 horses. J. Am. Vet. Med. Assoc. 224 (2) pp. 254-263.

– Kuemmerle, J.M., Auer, J.A., Rademacher, N., Lischer, C.J., Bettschart- Wolfensberger, R. and Fürst, A.E. (2008) Short incomplete sagittal fractures of the proximal phalanx in ten horses not used for racing. Vet. Surg. 37, pp.193-200.

– Lanyon LE. (1987) Functional strain in bone tissue as an objective, and controlling stimulus for adaptive bone remodelling. J Biomech 20, pp1083–1093.

– Lipreri, G.L., Bladon, B.M., Giorio, M.E., Singer, E.R. (2018) Conservative versus surgical treatment of 21 sports horses with osseous trauma in the proximal phalangeal sagittal groove diagnosed by low-field MRI. Veterinary Surgery, 47, pp. 908-915.

– Lopez, M.J. (2019) Bone biology and fracture healing. In: ”Equine Surgery”. Eds: Auer J.A and Stick J.A. 5th ed. Elsevier, Sounders, St Louis, Missouri.

– Manolagas, S.C. (2000) Birth and death of bone cells: basic regulatory mechanisms and implications for the pathogenesis and treatment of osteoporosis. Endocr. Rev., 21, pp. 115-137.

– Margulies, J.Y., Simkin, A., Leichter, I. et al. (1986) Effect of intense physical activity on the bone-mineral content in the lower limbs of young adults. J Bone Joint Surg Am. 68, pp. 1090-1093.

– Markel, M.D. and Richardson, D.W. (1985) Noncomminuted fractures of the proximal phalanx in 69 horses. J. Am. Vet. Med. Assoc. 186, pp.573-579.

– Martin, B. (1995) Mathematical model for repair of fatigue damage and stress fracture in osteonal bone. J Orthop Res. 13, pp. 309–316.

1961 – Martinelli, M.J. and Arthur, R.M. (2003) The American Thoroughbred. In: Equine
1962 Scintigraphy, Eds: S.J. Dyson, R.C. Pilsworth, A.R. Twardock and M.J. Martinelli,
1963 Equine Veterinary Journal Ltd, Newmarket, UK. pp149-150.
1964 – Martig, S., Chen, W., Lee, P.V.S. and Whitton, R.C. (2014) Bone Fatigue and its implications
1965 for injuries in racehorses. Equine Vet. J. 46, pp. 408-415.
1966 – Martig, S., Hitchens, P.L., Lee, P.V.S., Whitton, R.C. (2020) The relationship between
1967 microstructure, stiffness and compressive fatigue life of equine subchondral bone. Journal
1968 of the Mechanical Behavior of Biomedical Materials. 101, pp. 1034-39
1969 – Mason, M.W., Skedros, J.G., Bloebaum, R.D. (1995) Evidence of strain-mode-related
1970 cortical adaptation in the diaphysis of the horse radius. Bone. 17(3) pp. 229–37.
1971 – McCalden, R.W., McGeough, J.A., Barker, M.B., Court-Brown, C.M. (1993) Age related
1972 changes in the tensile properties of cortical bone. J Bone Joint Surg. 75A(8) pp.1193–205.
1973 – McCarthy, R.N., Jeffcott, L.B. (1992) Effects of treadmill exercise on cortical bone in the
1974 third metacarpus of young horses. Res Vet Sci 52 pp.28-27.
1975 – Merritt, J.S., Davies, H.M.S., Burvill, C.R., Pandy, M.G. (2008). Influence of muscle-
1976 tendon wrapping on calculations of joint reaction forces in the equine distal forelimb. Journal
1977 of Biomedicine and Biotechnology. Pp. 1-9.
1978 – Muir, P., McCarthy, J., Radtke, C.L., Markel, M.D., Santschi, E.M., Scollay, M.C., et al.,
1979 (2006). Role of endochondral ossification of articular cartilage and functional adaptation of
1980 the subchondral plate in the development of fatigue microcracking of joints. Bone. 38, pp.342–
1981 349
1982 – Murray, R.C., Whitton, R.C., Vedi, S., et al. (1999) The effect of training on the calcified
1983 zone of equine middle carpal articular cartilage. Equine Vet. J. Supplement 30, pp. 274–278.

1984 – Nixon A.J. (2019) Phalanges and the Metacarpophalangeal and Metatarsophalangeal
1985 joints. In: “Equine Surgery”. Eds: Auer J.A and Stick J.A. 4th ed. Elsevier, Sounders, St Louis,
1986 Missouri.
1987 – Noble, P., Singer, E.R., Nathan J.S. (2016) Does subchondral bone of the equine
1988 proximal phalanx adapt to race training? J. Anat. 229, pp. 104-113.
1989 – Norrdin, R.W., Stover, S.M., (2006). Subchondral bone failure in overload arthrosis: a
1990 scanning electron microscopic study in horses. J. Musculoskelet. Neuronal Interact. 6, pp.251–
1991 257.
1992 – O’Brien, F.J., Hardiman, D.A., Hazemberg, J.G. et al. (2005) The behaviour of
1993 microcracks in compact bone. Eur. J. Morphol. 42, pp. 71-79.
1994 – O'Hare, L.M.S., Cox, P.G., Jeffery, N., Singer, E.R. (2013) Finite element analysis of stress
1995 in the equine proximal phalanx. Equine Vet. J. 45(3), pp. 273–277.
1996 – Palmer, J.L. and Bertone, A.L. (1996) Joint biomechanics in the pathogenesis of
1997 traumatic arthritis. In: “Joint Disease in the Horse”. Eds: C.W. McIlwraith and G.W. Trotter,
1998 W.B. Saunders Co., Philadelphia. pp 104-119.
1999 – Parks, A. (2003) Form and function of the equine digit. Vet Clin Equine 19, pp.285–307.
2000 – Parkin, T., French, N., Riggs, C., Morgan, K., Clegg, P., Proudman, C., Singer, E.R. and
2001 Webbon, P.M. (2004) Risk of fatal distal limb fractures among thoroughbreds involved in the
2002 five types of racing in the United Kingdom. Vet. Rec. 154, pp.493-497.
2003 – Parkin T.D., Clegg P.D., French N.P., et al. (2005) Risk factors for fatal lateral condylar
2004 fracture of the third metacarpus/ metatarsus in UK racing. Equine Vet. J. 37(3), pp. 192-199.
2005 – Peloso, J.G., Vogler Iii, J.B., Cohen, N.D., Marquis, P. and Hilt, L. (2015) Association of
2006 catastrophic biaxial fracture of the proximal sesamoid bones with bony changes of the

2007 metacarpophalangeal joint identified by standing magnetic resonance imaging in cadaveric
2008 forelimbs of Thoroughbred racehorses. J. Am. Vet. Med. Ass. 246, 661-673.
2009 – Powell, S.E. (2012) Low-field standing magnetic resonance imaging findings of the
2010 metacarpo/metatarsophalangeal joint of racing Thoroughbreds with lameness localised to the
2011 region: a retrospective study of 131 horses. Equine Vet. J. 44, pp.169-177
2012 – Prendergast, P.J., Taylor, D. (1994) Prediction of bone adaptation using damage
2013 accumulation. Journal of biomechanics. 27(8), pp. 1067-1076.
2014 – Ramzan PHL, Powell SE. (2010) Clinical and imaging features of suspected prodromal
2015 fracture of the proximal phalanx in three Thoroughbred racehorses. Equine Vet J. 42(2):164-
2016 169.
2017 – Ramzan, P.H.L. and Palmer, L. (2011) Musculoskeletal injuries in Thoroughbred
2018 racehorses: a study of three large training yards in Newmarket, UK (2005–2007). Vet. J. 187,
2019 pp325-329.
2020 – Richardson, D.W. and Dyson, S.J. (2011) The Metacarpophalangeal joint. In: "Diagnosis
2021 and Management of Lameness in the Horse". Eds: Ross, M.W. and Dyson, S.J. 2nd ed. Elsevier
2022 Sounders, St. Louis, Missouri.
2023 – Riggs, C.M., Vaughan, L.C., Evans, G.P., et al. (1993) Mechanical implications of collagen
2024 fibre orientation in cortical bone of the equine radius. Anatomy and embryology. 187(3) pp.
2025 239–48.
2026 – Riggs, C.M., Whitehouse, G.H. and Boyde, A. (1999) Pathology of the distal condyles of the
2027 third metacarpal and third metatarsal bones of the horse. Equine Vet. J. 31, pp. 140-148.
2028 – Robling, A.G. and Bonewald, L.F. (2020) The osteocyte: new insights. Annu. Rev.
2029 Physiol. 82 pp. 485-506.
2030 – Rubin, C.T. and Lanyon, L.E. (1984) Regulation of bone formation by applied dynamic

loads. The Journal of bone and joint surgery. American volume. 66(3), pp. 397-402.

– Rubio-Martinez, L.M., Cruz, A.M., Gordon, K., Hurtig, M.B., (2008). Structural characterization of subchondral bone in the distal aspect of third metacarpal bones from Thoroughbred racehorses via micro-computed tomography. Am. J. Vet. Res. 69, pp.1413–1422

– Rubio-Martínez, L.M., Cruz, A.M., Gordon, K. and Hurtig, M.B. (2008) Mechanical properties of subchondral bone in the distal aspect of third metacarpal bones from Thoroughbred racehorses. Am. J. Vet. Res. 69, pp.1423-1433.

– Ruggle, A.J. (2011) The proximal and middle phalanges and interphalangeal joint. In: "Diagnosis and Management of Lameness in the Horse". Eds: Ross, M.W. and Dyson, S.J. 2nd ed. Elsevier Sounders, St. Louis, Missouri.

– Schaffler, M.B., Cheung, W-Y., Majeska, R. and Kennedy, O. (2014) Osteocytes: master orchestrator of bone. Calcif. Tissue Int. 94, pp. 5-24.

– Sims, N.A. and Martin, T.J. (2019) The osteoblast lineage: its actions and communication mechanisms. In: "Principles of Bone Biology". Eds: Bilezikian, J.P., Martin, T.L., Clemens, T.L. and Rosen, C.J. 4th ed. Elsevier Academic Press.

– Sinclair, C., Birch, H.L., Smith, R.K.W., Goodship, A.E. (2014) Skeletal physiology: responses to exercise and training. In: "Equine Sports Medicine and Surgery". Eds. Hinchcliff, K.W., Kaneps, A.J., Geor, R.J. 2nd ed. Elsevier.

– Singer, E.R., Garcia, T., Stover, T. (2013) How do metacarpophalangeal joint extension, collateromotion and axial rotation influence dorsal surface strains of the equine proximal phalanx at different loads in vitro? Journal of Biomechanics. 46, pp. 738–744

2053 – Smith, M. and Wright, I.M. (2014a) Radiographic configuration and healing of 121
2054 fractures of the proximal phalanx in 120 Thoroughbred racehorses (2007–2011). Equine Vet.
2055 J. 46, pp. 81-87.
2056 – Smith, M. and Wright, I.M. (2014b) Are there prodromal changes with proximal
2057 phalangeal parasagittal fractures? Equine Vet. J. 46, pp. 88-91.
2058 – Smith, M., Corletto, F.C., Wright, I.M. (2017) Parasagittal fractures of the proximal
2059 phalanx in Thoroughbred racehorses in the UK: Outcome of repaired fractures in 113 cases
2060 (2007–2011). Equine Vet. J. 49 (6), pp. 784–788.
2061 – Stover, S.M. and Murray, A. (2008) The California *Postmortem Program*: leading the
2062 way. Vet. Clin. N. Am: Equine Pract. 24, pp. 21-36.
2063 – Takahashi, N., Kobayashi, Y. and Udagawa, N. (2019) Osteoclasts. In: In: "Principles of
2064 Bone Biology". Eds: Bilezikian, J.P., Martin, T.L., Clemens, T.L. and Rosen, C.J. 4th ed. Elsevier
2065 Academic Press.
2066 – Taylor, D., Casolari, E. and Bignardi, C. (2004) Predicting stress fractures using a
2067 probabilistic model of damage, repair and adaptation. J. Orthop. Res. 22, pp. 487-494.
2068 – Tetens, J., Ross, M.W. and Lloyd, J.W. (1997) Comparison of racing performance before
2069 and after treatment of incomplete, midsagittal fractures of the proximal phalanx in
2070 standardbreds: 49 cases (1986–1992). J. Am.Vet. Med. Assoc. 210, pp. 82-86.
2071 – Turner , C.H. (1992) On Wolff's law of trabecular architecture. J Biomech. 25, pp1–9.
2072 – Verborgt, O., Gibson, G.J., Schaffler, M.,B. (2000) Loss of osteocyte integrity in
2073 association with microdamage and bone remodeling after fatigue in vivo. Journal of bone and
2074 mineral research: the official journal of the American Society for Bone and Mineral Research
2075 15(1), pp. 60–67.

– Verheyen, K.L.P. and Wood, J.L.N (2004) Descriptive epidemiology of fractures occurring in British Thoroughbred racehorses in training. Equine Vet. J. 36(2) pp.167-173.
– Wallace, J.M. (2014). Scheletal Hard Tissue Biomechanics. In: Basic and applied bone biology. Burr, D.B. and Allen, M.R. Ed. Elsevier, pp. 115-130.
– Wang, X., Thomas, C.D., Clement, J.G. et al. (2016) A mechanostatistical approach to cortical bone remodelling: an equine model. Biomech. Model. Mechanobiol. 15, pp. 29-42.
– Whitton, R.C., Trope, G.D., Ghasem-Zadeh, A., Anderson, G.A., Parkin, T.D.H., Mackie, A., Seeman, E. (2010) Third metacarpal condylar fatigue fractures in equine athletes occur within previously modelled subchondral bone, Bone. 47, pp. 826–831
– Whitton, R.C., Mirams, M., Mackie, E.J., Anderson, G.A. and Seemain, E. (2013) Exercise-induced inhibition of remodelling is focally offset with fatigue fracture in racehorses. Osteoporos. Int. 24, pp. 2043-2048.
– Whitton, R.C., Ayodele, B.A., Hitchens, P.L., Mackie, E.J., (2018) Subchondral bone microdamage accumulation in distal metacarpus of Thoroughbred racehorses. Equine Vet. J. 50, pp.766–773.
– Young, D.R., Nunamaker, D.M. and Markel, M.D. (1991) Quantitative evaluation of the remodeling response of the proximal sesamoid bones to training-related stimuli in thoroughbreds. Am. J. Vet. Res. 52, p.1350.